Electronic Supplementary Material (ESI) for Journal of Materials Chemistry A.

# Electronic Supplementary Information

## Fixed-Bed Photoreactor using Conjugated Nanoporous Polymer-Coated Glass Fibers for Visible Light-promoted Continuous Photoredox Reactions

Wei Huang, Beatriz Chiyin Ma, Di Wang, Zi Jun Wang, Run Li, Lei Wang, Katharina Landfester, and Kai A. I Zhang*

*Max Planck Institute for Polymer Research, Ackermannweg 10, D-55128 Mainz, Germany, E-mail: kai.zhang@mpip-mainz.mpg.de*

### Materials

1,3,5-triethylbenzene, 4,7-dibromobenzo[c][1,2,5]thiadiazole, $Pd(PPh3)_2Cl_2$ and CuI were purchased from Sigma Aldrich. Glass fiber was purchased from Carl Roth. All the reactants and solvents were used without further purification. MacMillan catalyst (2R,5S)-2-tertbutyl-3,5-dimethylimidazolidin-4-one • HCl was synthesized according to the literature.[1-2] The comparison sample g-$C_3N_4$ was synthesized according to literature.[3]

### Characterizations

UV-vis absorption spectra were recorded at room temperature on a Perkin Elmer Lambda 100 spectrophotometer. $^1H$ and $^{13}C$ NMR measurements were conducted on Bruker AVANCE 250 and Bruker AVANCE 300 systems. FT-IR spectra were recorded on a Varian 1000 FT-IR spectrometer. Solid State $^{13}C$ CP/MAS NMR measurements were carried out using Bruker Avance II solid state NMR spectrometer operating at 300 MHz Larmor frequency equipped with a standard 4mm magic angle spinning (MAS) double resonance probe head. Scanning electron microscope (SEM) images were recorded on a LEO Gemini 1530 (Carl Zeiss AG, Germany) using an in lens SE detector. The thermal gravity analysis (TGA) measurement was conducted under nitrogen with temperature increasing from 25 °C to 800 °C at a rate of 10 °C/min. BET surface areas and pore size distributions were measured by nitrogen adsorption and desorption at 77 K using Autosorb 1 (Quantachrome Instruments). Samples were degassed at 150 °C for 24 h under high vacuum before analysis. The BET surface area calculation was based on data points obtained from $0<P/P_0<0.25$ and the nonlinear density functional theory (NLDFT) equilibrium model was used for the BET model fitting. Pore size distributions and pore volumes were derived from the adsorption branches of the isotherms using Quenched Solid Density Functional Theory (QSDFT, N2, assuming carbon adsorbent with slit pores). Cyclic voltammetry (CV) measurement was performed using an Autolab PGSTAT204 potentiostat/galvanostat (Metrohm). A glassy carbon electrode was as the working electrode covered with a thin polymer film via drop-casting. A Pt wire was used as the counter electrode and a Hg/HgCl (in saturated KCl solution) electrode was used as the reference electrode. $Bu_4NPF_6$ (0.1 M in acetonitrile) was used as electrolyte solution. The reduction potential was recorded with a scan rate of 100 mV/s. The EPR spectra were recorded on a Bruker EMX-plus spectrometer equipped with an NMR gauss meter and a variable-temperature control continuous-flow-$N_2$ cryostat (Bruker B-VT 2000).

### Fabrication of B-BT-coated glass fibers

The glass fibers were first cleaned with piranha solution ($H_2O_2$: $H_2SO_4$ = 1:3) to remove the surficial contaminants. Then the glass fibers (600 mg), $Pd(PPh_3)_2Cl_2$ (7 mg, 0.01 mmol) and CuI (2 mg, 0.01 mmol), N,N-dimethylformamide (DMF) and trimethylamine (40 ml, 1:1, v/v)was added into a 100 ml flask, followed by ultrasonic treatment for 1 hour under nitrogen. Subsequently, a solution of triethynylbenzene (12 mg, 0.08 mmol) and 4,7-dibromobenzo[c][1,2,5]thiadiazole (30 mg, 0.1 mmol) dissolved in 5 ml DMF was added under slight shaking. The reaction mixture was then heated at 90 $^oC$ for 24 hours without stirring under nitrogen. After cooling down to room temperature, the obtained bright yellow glass fibers were washed with water, methanol, acetone and extracted in a Soxhlet with dichloremethane and methanol (1:1) for 24 hours, then dried under vacuum at 80 $^oC$ overnight.

### Photocatalytic dehalogenation in the fix-bed photoreactor

200 mg B-BT-coated glass fibers were loosely packed into a transparent glass tube (Ominifit, r = 0.35 cm, L = 7 cm) end-capped with two frits, equipped with PTFE-tubing (*d* = 8 mm). 1 mmol substrate, 1.1 mmol Hantzsch ester and 2 mmol diisopropylethylamine was added into 10 ml DMF and then was continuously pumped through the column under nitrogen atmosphere for 2 hour. Simultaneously, the column was irradiated with a white light LED lamp (OSA Opto Lights, 4.5 mW/cm$^2$, $\lambda$>420 nm). Samples were taken out directly from the output with a syringe and the conversion was determined by $^1H$ NMR.

### Photocatalytic α-alkylation of aldehydes

The same fix-bed photoreactor as for the dehalogenation was used. In a typical procedure, a reaction mixture containing α-bromo-carbonyl compound (1.6 mmol), aldehyde (3.2 mmol), 2,6-lutidine 375 µl, 3.2 mmol) and (2R,5S)-2-tertbutyl-3,5-dimethylimidazolidin-4-one×TfOH (66 mg, 0.32 mmol) in 10 ml DMF was pumped through the column continuously under nitrogen atmosphere for a predetermined time. The column was irradiated with a blue light LED lamp (OSA Opto Lights, 4.5 mW/cm$^2$, λ>420 nm). Samples were taken out directly from the output with a syringe and the conversion was determined by $^1$H NMR. Enantioselectivity was estimated according to the literature.[4]

## Synthesis of the monolith m-B-BT

A modified protocol as reported in the literature was used.[5] Triethynylbenzene (82 mg, 0.5 mmol) and 4,7-dibromobenzo[c][1,2,5]thiadiazole (240 mg, 0.8 mmol) were dissolved in 7.5 ml pyrrolidine with moderate heating. Then 10 mg $PdCl_2$ in 7.5 ml Milli-Q water was added with vigorous stirring for 30 min. Then the mixture was transferred into a Teflon-lined autoclave and heated up to 150 °C under N2 for 10 hours. The formed monolith product was carefully washed with water, ethanol and extracted with tetrahydrofuran and dichloromethane in a Soxhlet extractor. The monolithic product was obtained after drying using supercritical $CO_2$.

## Turnover frequency (TOF)

The turnover frequency (TOF) can be used to quantify the reaction rate. Herein, for heterogeneous photocatative system, the TOF could be defined with respect to the catalyst weight as:

$$\text{TOF}=\frac{[\text{reacted substrate (mol)}]}{[\text{reaction time (h)}]\times[\text{photocatalyst weight (g)}]}$$

The TOF value of the dehalogenation of α-bromoacetophenones was calculated to be 0.08 mol $h^{-1}$ $g^{-1}$, and for the model reaction α-alkylation of the 3-phenylpropylaldehyde and α-bromomalonate (Entry 1 in Table 1) was determined to be 0.021 mol $h^{-1}g^{-1}$.

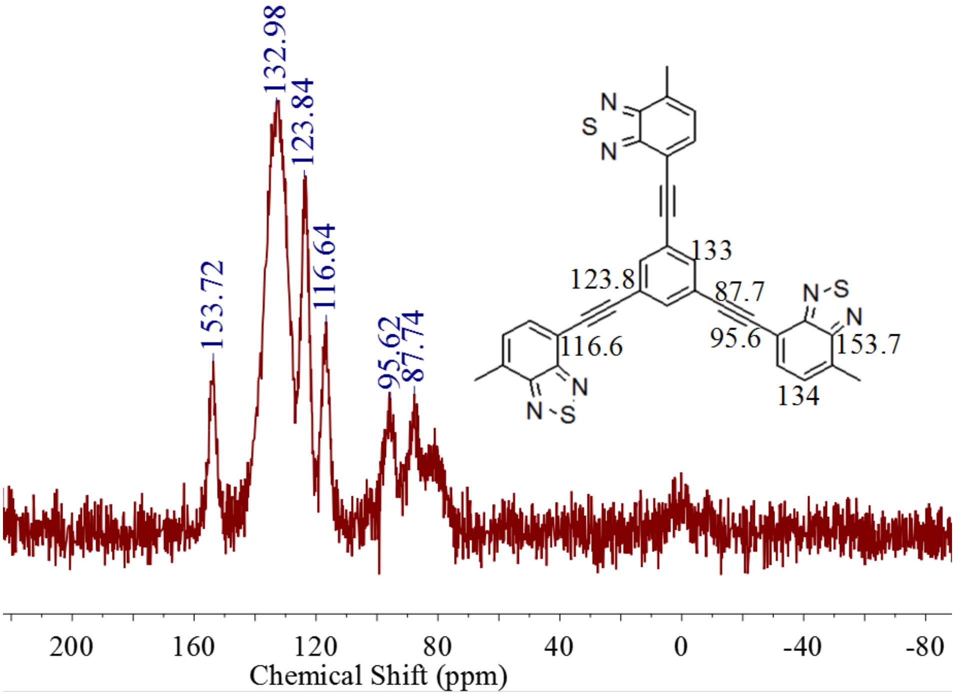

**Figure S1.** Solid State $^{13}$C CP/MAS NMR spectrum of B-BT.

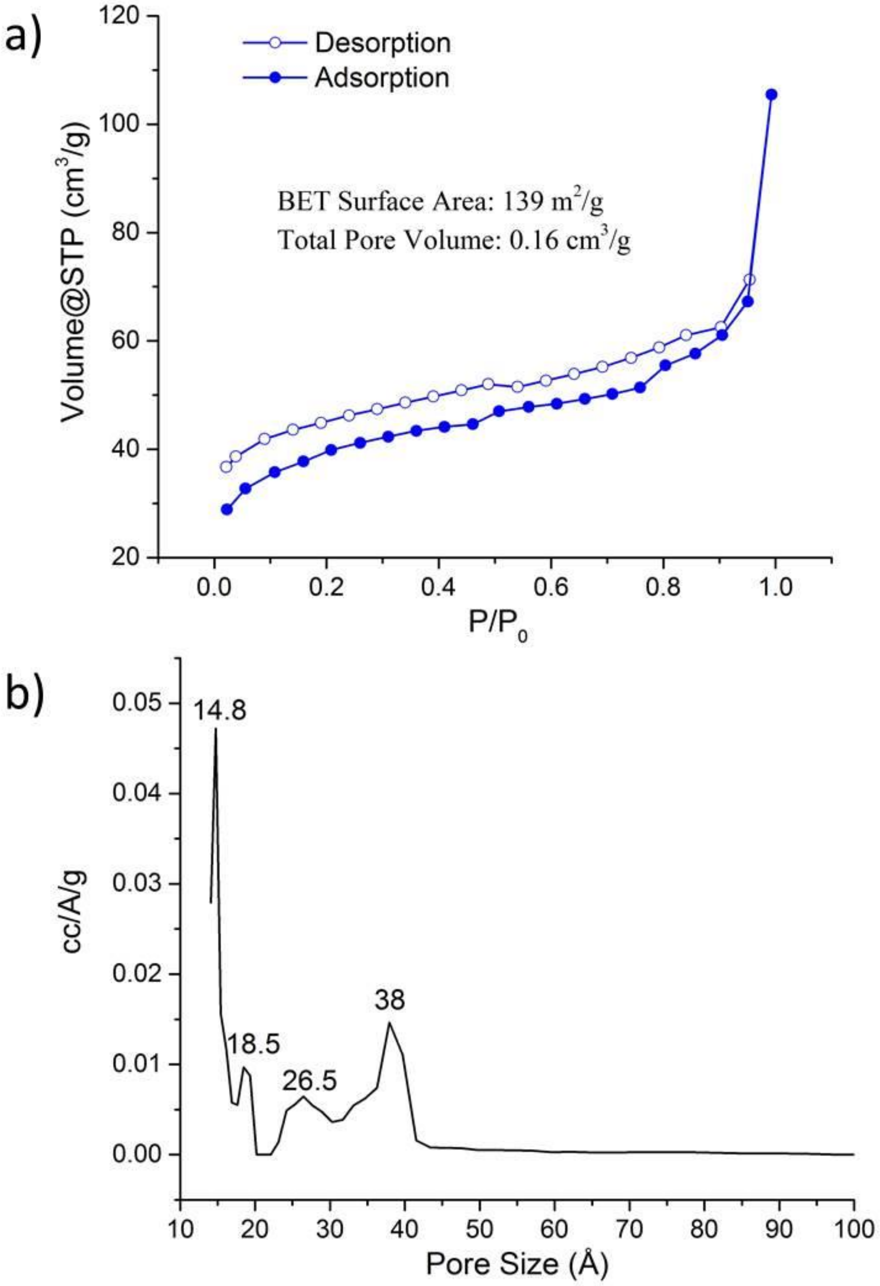

**Figure S2.** $N_2$ gas absorption-desorption isotherm of B-BT measured at 77 K and (b) pore size distribution.

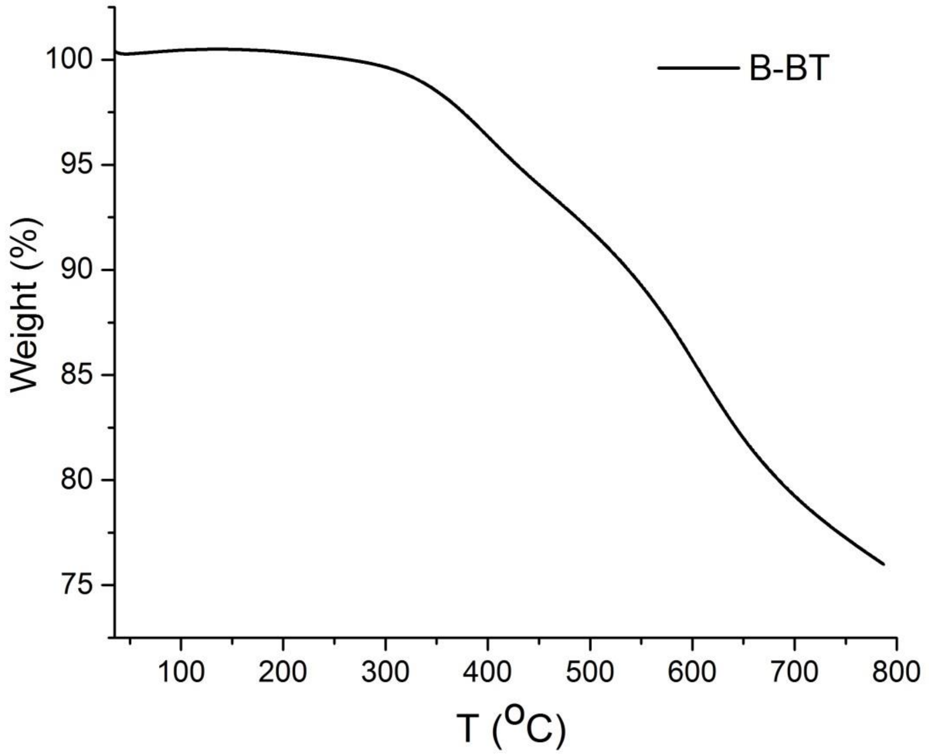

**Figure S3.** TGA curve of pure B-BT under nitrogen atmosphere.

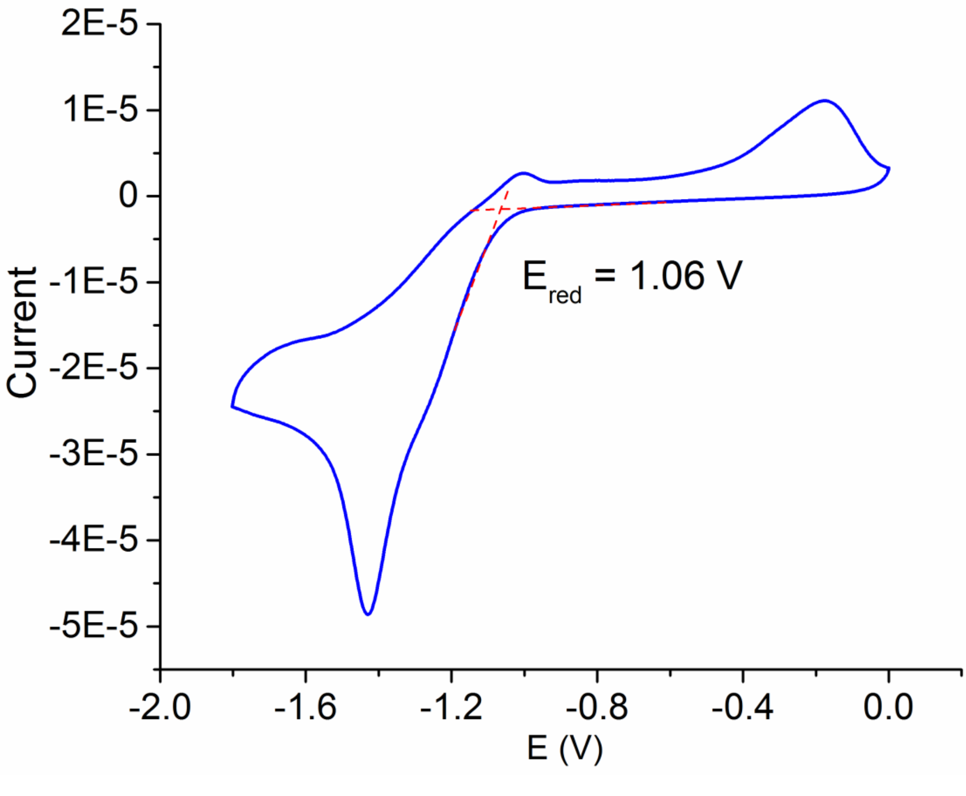

**Figure S4.** Cyclic voltammetry measurement of B-BT (reductive cycle).

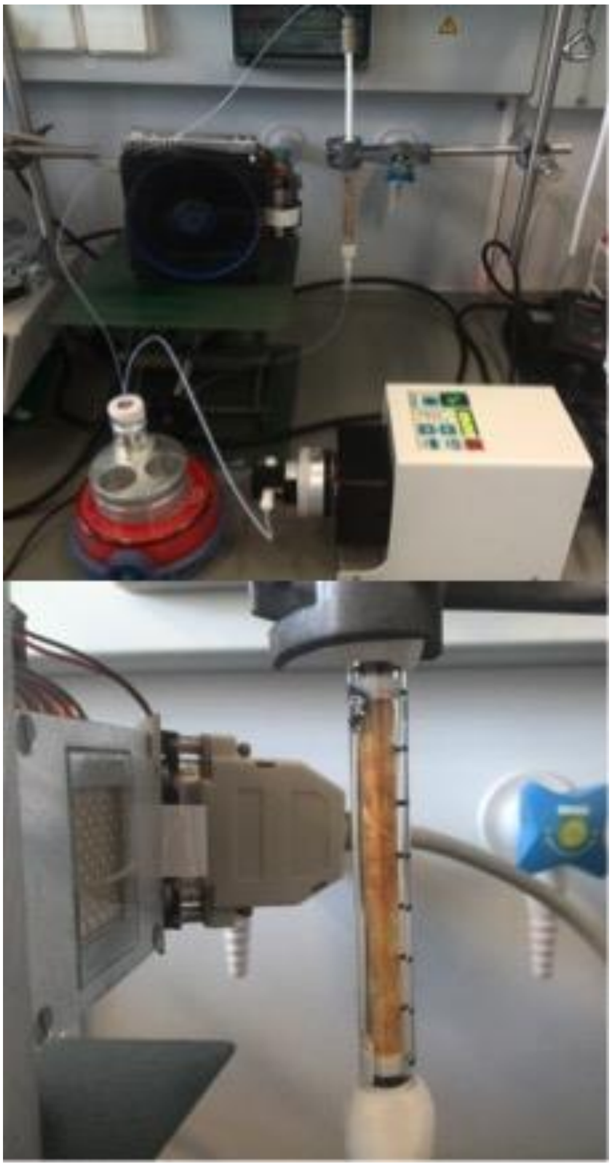

**Figure S5.** Setup of the fix-bed photoreactor in the continuous flow system.

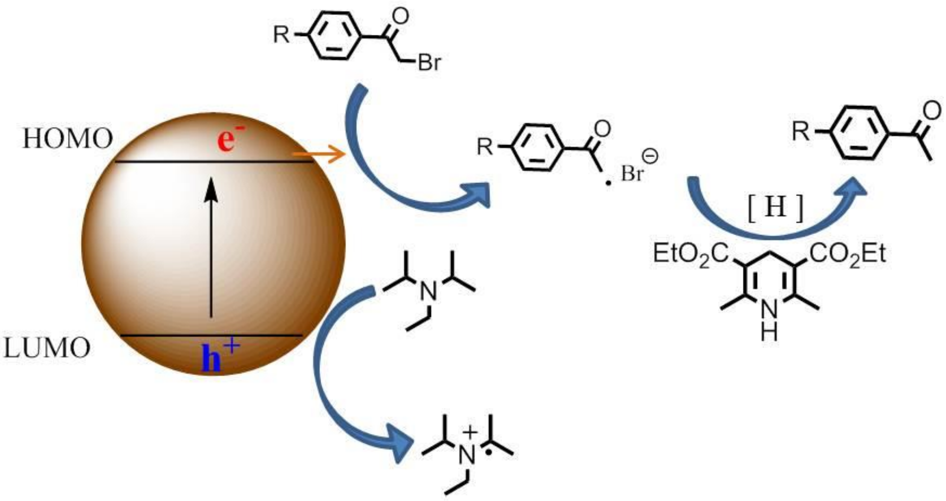

**Figure S6.** Reaction mechanism of the visible light-driven dehalogenation reaction.

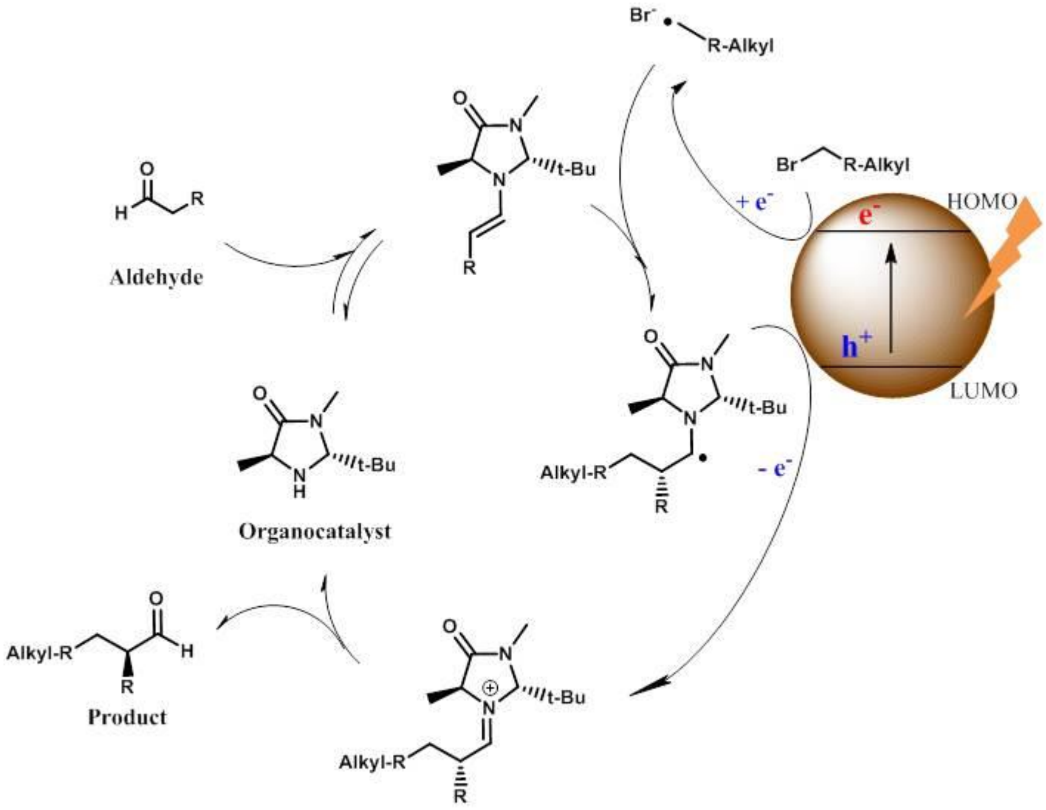

**Figure S7.** Proposed photocatalytic mechanism of the α-alkylation of aldehydes with conjugated nanoporous polymer as photocatalyst.

The formation of malonate alkyl radical and acetophenone radical were recorded by electron paramagnetic (EPR) measurement in a DMF solution of α-bromo-carbonyl compound (0.5M), photocatalyst B-BT (1 mg/ml) in the presence of N-tert-butyl-α-phenylnitrone (PBN) (0.1 M) as a radical trap. EPR signals with a characteristic doublet of triplets were observed under irradiation by visible light, which is typical for PBN adduct of alkyl radical having carbonyl groups in α-position.[6]

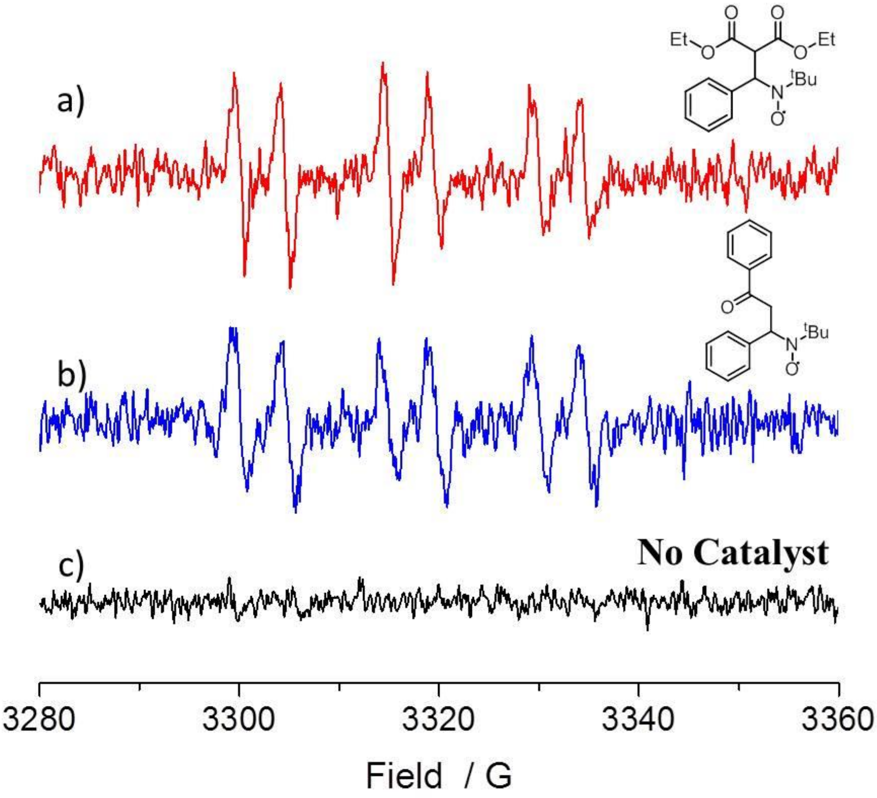

**Figure S8.** EPR spectra of spin adducts of a) malonate alkyl radical with PBN ($a_N$=15.1 G, $a_H$=4.9 G, g=2.006); acetophenone radical with PBN ($a_N$=15.5 G, $a_H$=5.1 G, g=2.0057) and c) without catalyst.

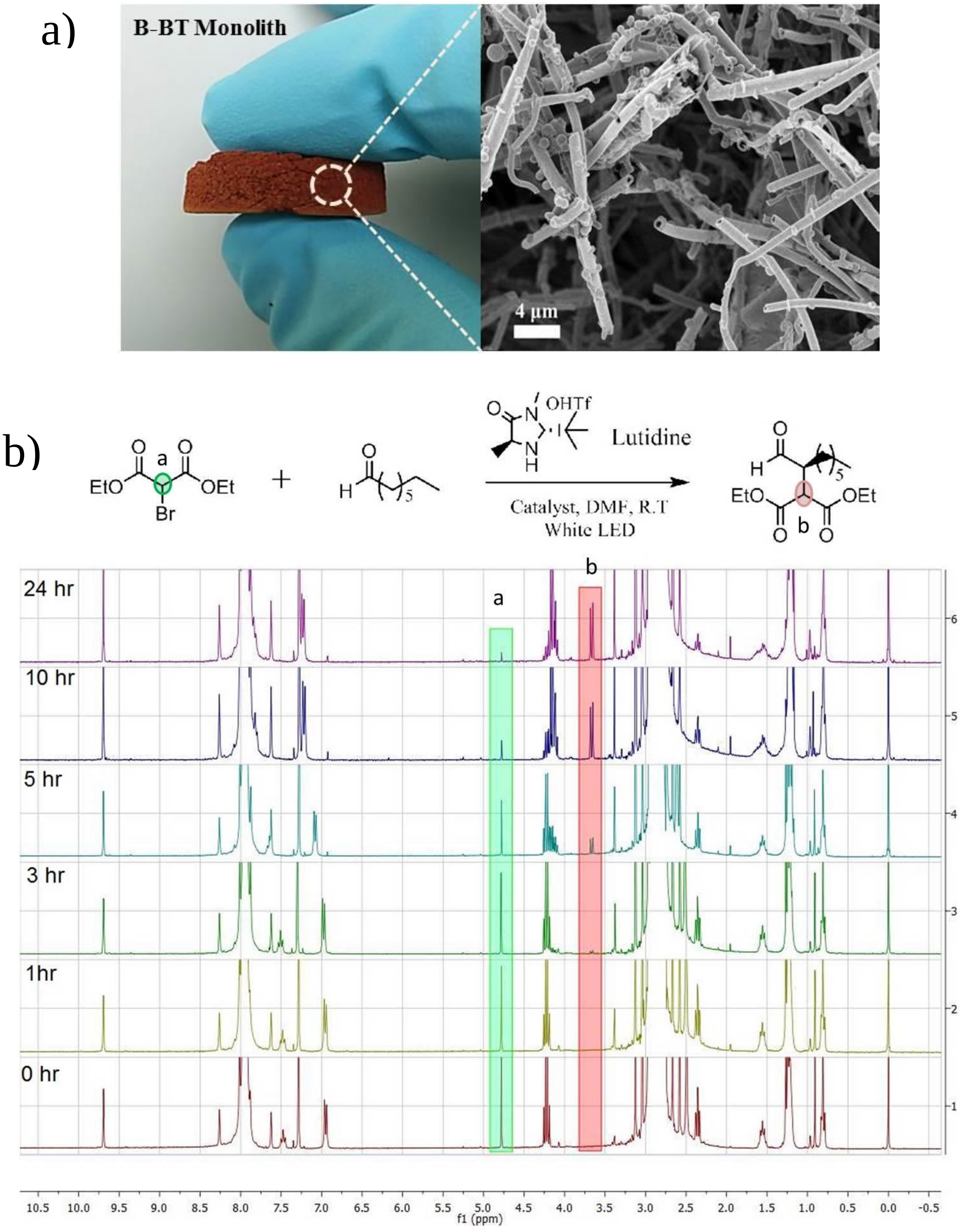

**Figure S9.** a) Photography of monolithic polymer m-B-BT and its SEM image; b) the monitoring experiment of the photocatalytic α-alkylation reaction of octanal with α-bromomalonate using the photoreactor containing m-B-BT using $^1$H NMR. Reaction conditions: m-B-BT (100 mg), α-bromomalonate (1.6 mmol), octanal aldehyde (3.2 mmol), 2,6-lutidine (375 µl, 3.2 mmol) and (2R,5S)-2-tertbutyl-3,5-dimethylimidazolidin-4-one×HCl (66 mg, 0.32 mmol), 10 ml DMF, white LED (λ>420 nm).

**NOTE1:** The intensity of the peak at ca. 4.8 ppm assigned to bromomalonate gradually attenuated with increasing reaction time, simultaneously, a double peak at ca. 3.66 ppm from the desired product increasingly enhanced, indicating the effective photocatalytic coupling reaction. The conversion was estimated to be 90.3 % after **24** hours based on the bromomalonate. In comparison, using B-BT coated glass fiber as catalyst (ca. 6.4 mg pure B-BT), a quantitative conversion was obtained after **5** hours (Table 1, Entry 6).

**NOTE2:** The formation mechanism of the microtubes inside the monolithic polymer m-B-BT is not fully understood yet. Similar morphology has been reported by Vilela *et al.* (ref. 42). We speculate that in the reaction medium, after adding amine into a non-solvent, in particular, water, the monomers could possibly form small crystals. The crystals could function as a kind of template. The microtube could grow on the template, which itself could be “consumed” during the microtube formation. And the thickness of the microtube could depend on the size of the monomer crystals and their concentration.

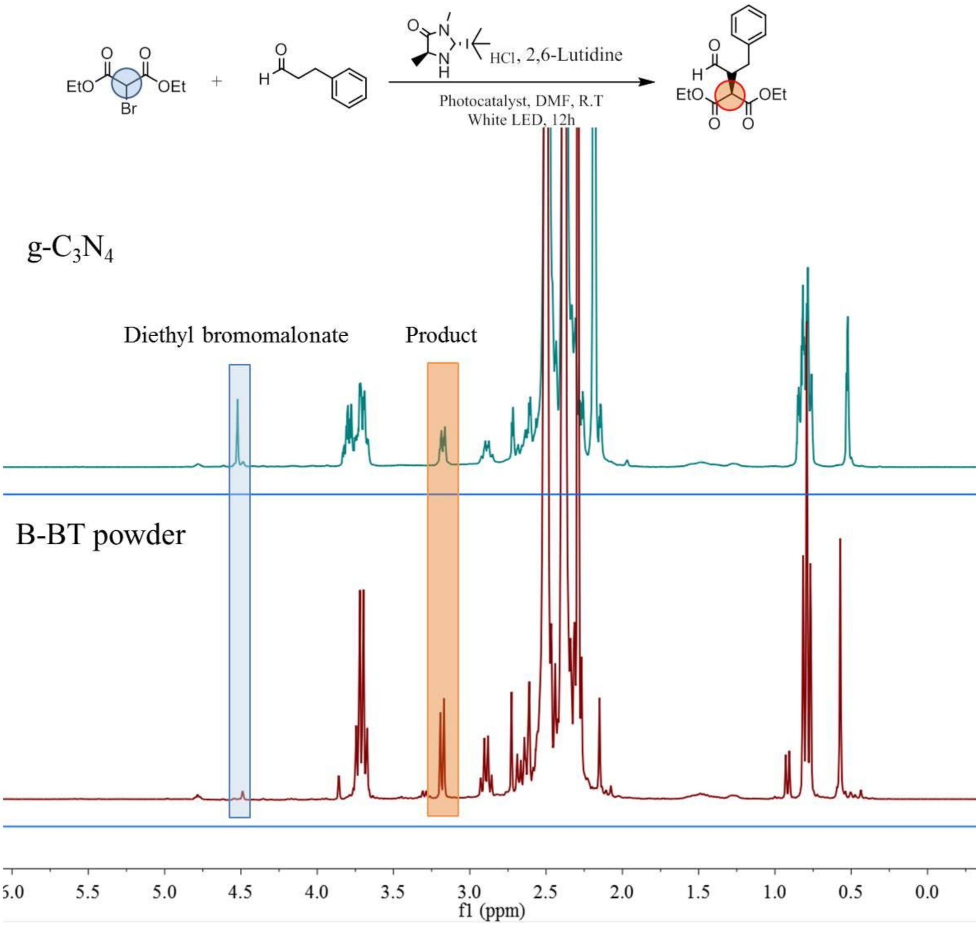

**Figure S10.** Comparison of the catalytic acitivity of g-C3N4 with powder-like B-BT-based photocatalyst using a model reaction of α-alkylation reaction of 3-phenylpropanal with α-bromomalonate. A conversion of 70.4 % was obtained for g-$C_3N_4$ after irradiation 12 hours under visible light (λ>420 nm), which is lower than that of the powder-like B-BT (95%).

**Table S1.** Temperature effect on the photocatalytic efficiency of the photoreactor under standard reaction conditions.

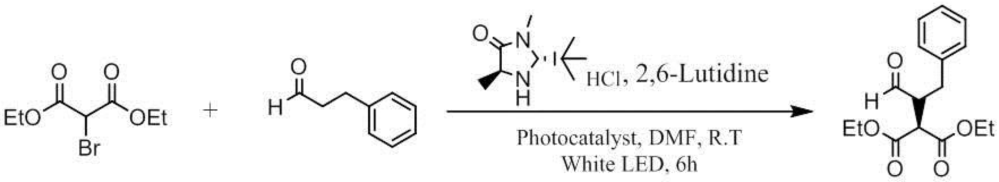

| **Reaction Temperature ($^o$C)** | **Reaction time (h)** | **Conversion (%)** |
|---|---|---|
| 0 | 6 | 82.6 |
| 25 | 6 | 84.0 |
| 50 | 6 | 85.1 |

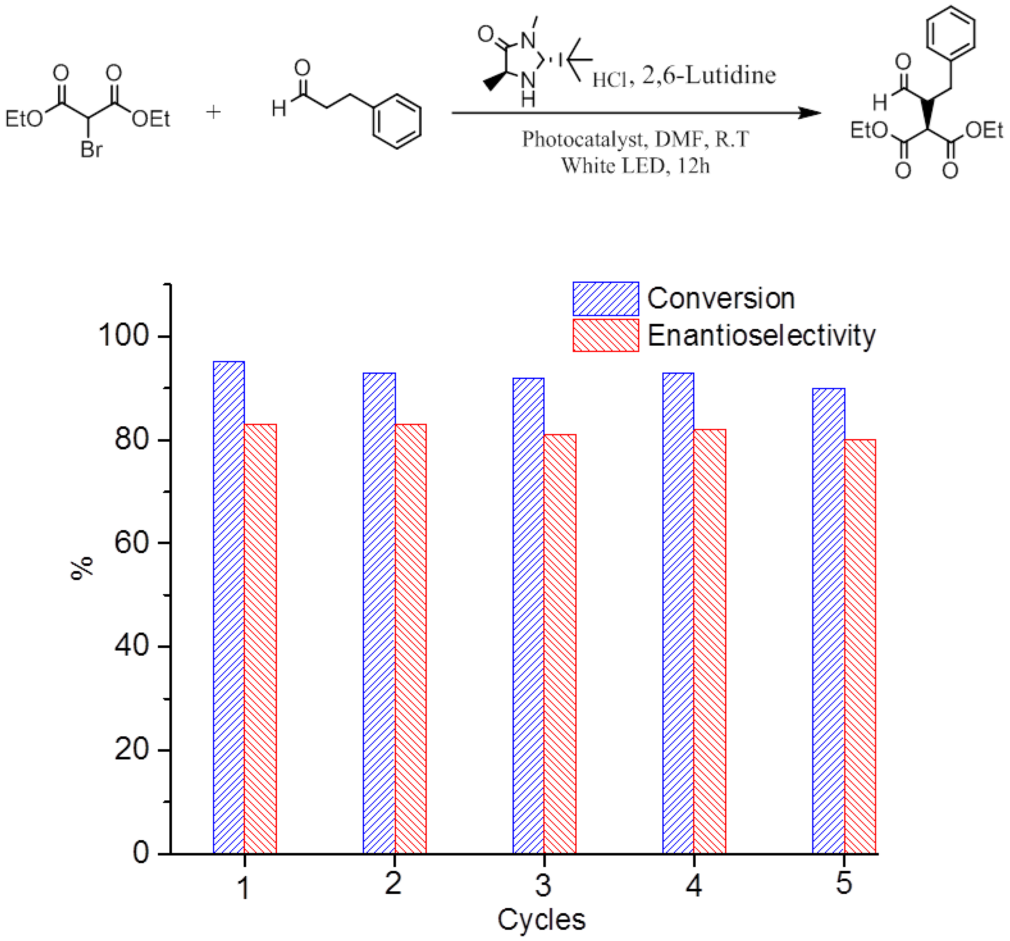

**Figure S11.** Repeating experiment of the enantioseletive α-alkylation reaction in the fix-bed photoreactor.

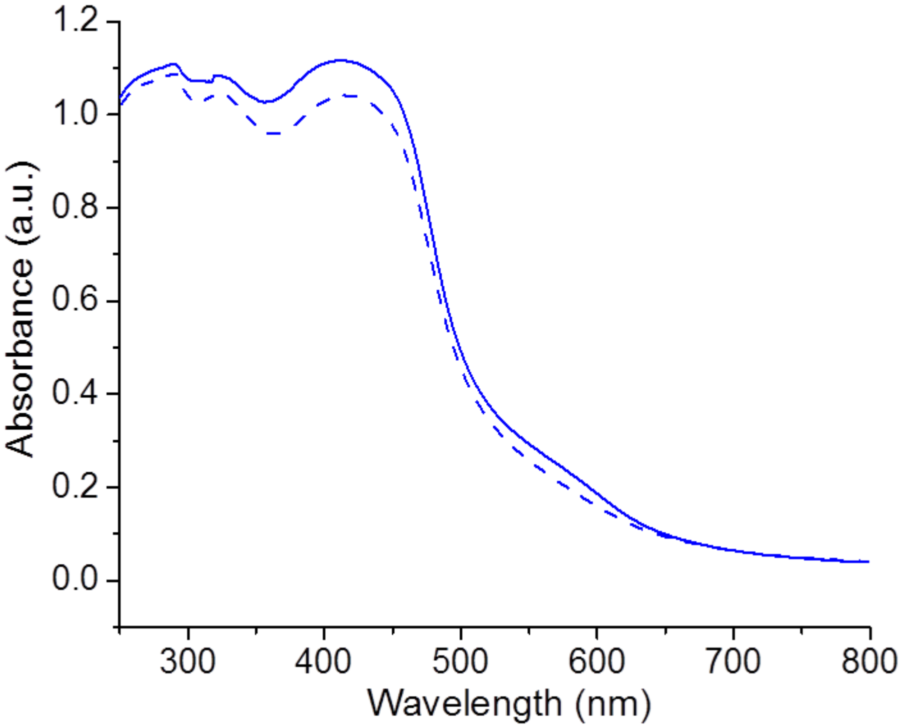

**Figure S12:** DR UV/vis spectra of the B-BT coated glass fibers before (solid line) and after (dash line) five repeating experiments.

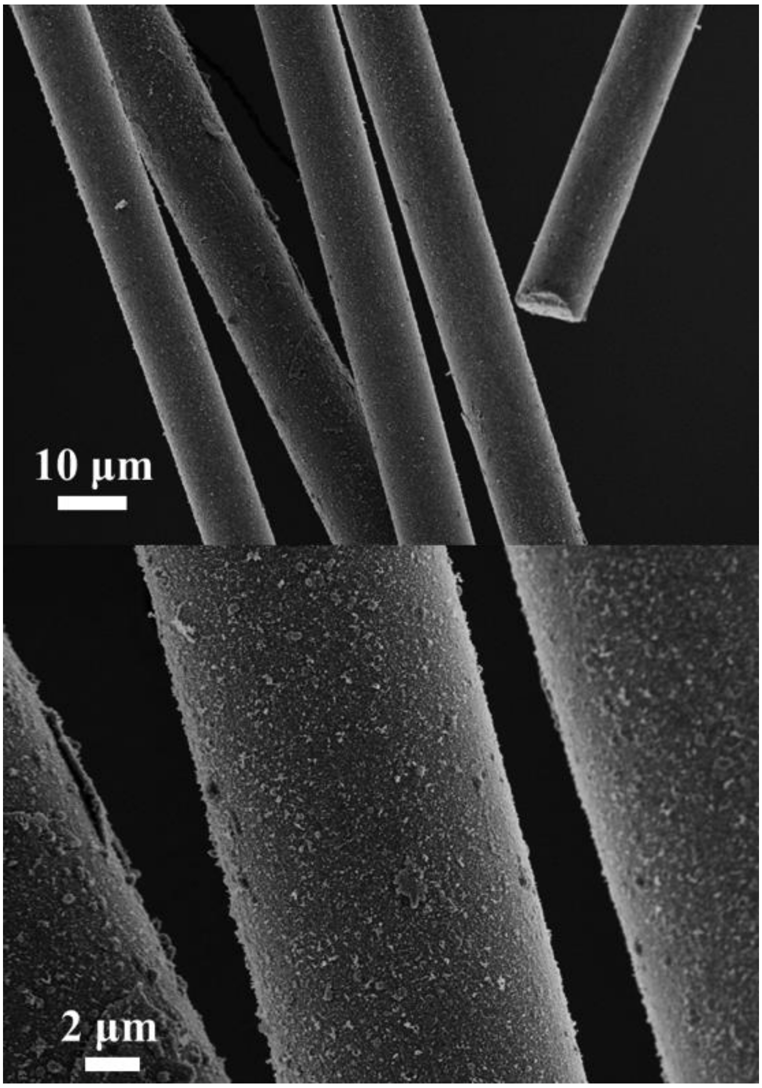

**Figure S13.** SEM images of B-BT-coated glass fibers after five repeating reaction cycles.

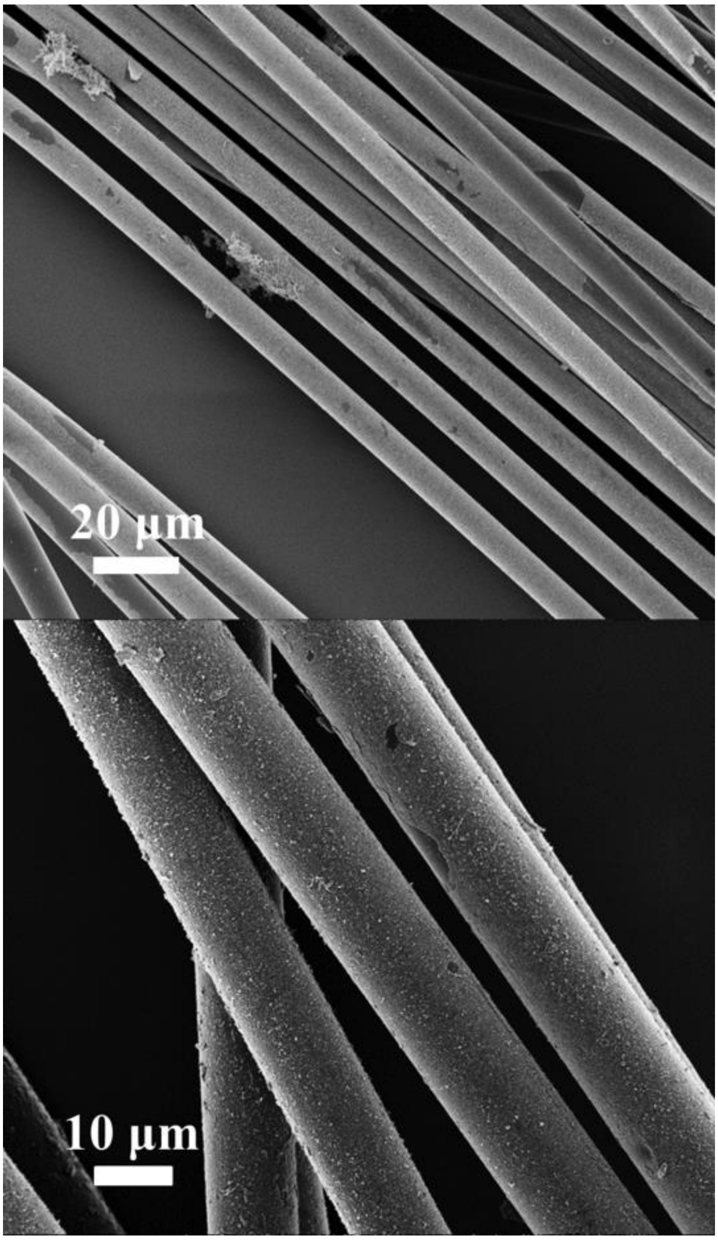

**Figure S14.** Additional SEM images of B-BT coated glass fibers.

[1] T. H. Graham, B. D. Horning, D. W. MacMillan, Org. Synth. 2011, 88, 42-53;

[2] A. Gualandi, M. Marchini, L. Mengozzi, M. Natali, M. Lucarini, P. Ceroni, P. G. Cozzi, ACS Catal. 2015, 5, 5927.

[3] J. Liu, Y. Liu, N. Liu, Y. Han, X. Zhang, H. Huang, Y. Lifshitz, S.-T. Lee, J. Zhong and Z. Kang, Science, 2015, 347, 970.

[4] D. A. Nicewicz and D. W. MacMillan, Science, 2008, 322, 77-80.

[5] J. Liu, J. M. Tobin, Z. Xu, F. Vilela, Polym. Chem. 2015, 6, 7251.

[6] A. Gualandi, M. Marchini, L. Mengozzi, M. Natali, M, Lucarini, P. Ceroni, P. G. Cozzi, ACS Catal., 2015, 5, 5927-5931.

**Experimental data of the products**

**Acetophenone**

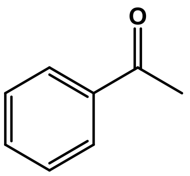

$^1$H NMR (300 MHz, $CDCl_3$) δ 7.90, 7.88 (d, 2H, Ar**H**), 7.50, 7.47 (d, 1H, Ar**H**), 7.42, 7.39, 7.36 (t, 2H, Ar**H**), 2.54 (s, 3H, -COC**H**$_3$); $^{13}$C NMR (300 MHz, $CDCl_3$) δ 198.1, 137.1, 133.1, 128.6, 128.3, 26.6

**4'-nitro-acetophenone**

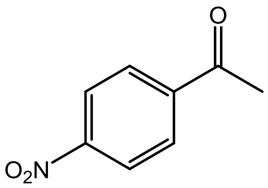

$^1$H NMR (300 MHz, $CDCl_3$) δ 8.27, 8.24 (d, 2H, Ar**H**), 8.06, 8.03 (d, 2H, Ar**H**), 2.62 (s, 3H, -COC**H**$_3$); $^{13}$C NMR (300 MHz, $CDCl_3$) δ 196.3, 150.4, 141.4, 129.3, 123.9, 27.0.

**4'-bromo-acetophenone**

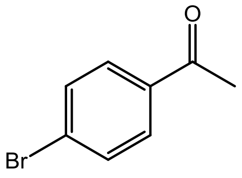

$^1$H NMR (300 MHz, $CDCl_3$) δ 7.77, 7.74 (d, 2H, Ar**H**), 7.56, 7.52 (d, 2H, Ar**H**), 2.52 (s, 3H, -COC**H**$_3$); $^{13}$C NMR (300 MHz, $CDCl_3$) δ 197.0, 135.8, 131.9, 129.8, 128.3, 26.5.

**4'-methoxyl-acetophenone**

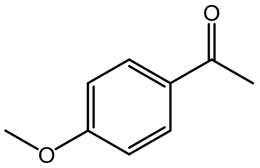

$^1$H NMR (300 MHz, $CDCl_3$) δ 7.89, 7.86 (d, 2H, Ar**H**), 6.89, 6.85 (d, 2H, Ar**H**), 3.81 (s, 3H, -OC**H**$_3$), 2.49 (s, 3H, -COC**H**$_3$); $^{13}$C NMR (300 MHz, $CDCl_3$) δ 196.8, 163.5, 130.6, 130.4, 113.7, 55.5, 26.4.

**Diethyl 2-(1-oxohexan-2-yl)propanedioate**

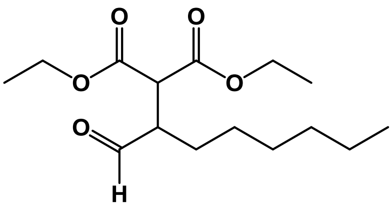

$^1$H NMR (300 MHz, $CDCl_3$) δ 9.70 (d,1H, C**H**O), 4.20-4.09 (m, 4H, 2×$CO_2$C**H**$_2$C$H_3$), 3.68,3.65 (d, 1H, C**H**(CO2Et)$_2$), 3.08-3.01 (m, 1H, C**H**CHO), 1.74-1.59 (m, 1H, C**H**$_2$($CH_2$)$_4$C$H_3$), 1.58-1.46 (m, 1H, C**H**$_2$($CH_2$)$_4$C$H_3$), 1.32-1.11 (m, 14H, C$H_2$(C**H**$_2$)$_4$C$H_3$, 2×$CO_2$C$H_2$C**H**$_3$), 0.83, 0.81, 0.78 (t, 3H,

$CH_2(CH_2)_4C\mathbf{H}_3$); $^{13}$C NMR (300 MHz, $CDCl_3$) δ 201.6, 168.1, 168.0, 61.8, 61.7, 51.8, 50.2, 31.4, 29.3, 27.1, 26.5, 22,5,14.0, 13.9.

**Diethyl 2-(1-oxo-3-phenylpropan-2-yl)propanedioate**

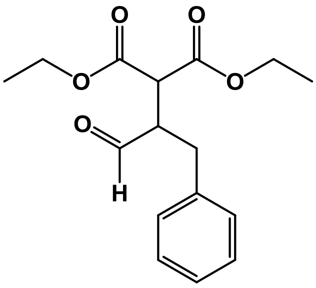

$^1$H NMR (300 MHz, CDCl3) δ 9.71 (s, 1H, C**H**O), 7.11-7.27 (m, 5H, Ar**H**), 4.09-4.17 (m, 4H, $2\times CO_2C\mathbf{H}_2CH_3$), 3.62, 3.60 (d, 1H, $C\mathbf{H}(CO_2Et)_2$), 3.28-3.35 (m, 1H, CHOC**H**), 3.02-3.09 (dd, 1H, $C\mathbf{H}_2$Ph), 2.72-2.80 (dd, 1H, $C\mathbf{H}_2$Ph), 1.18, 1.20, 1.22 (t, 6H, $2\times CO_2CH_2CH_3$); $^{13}$C NMR (300 MHz, $CDCl_3$) δ 201.1, 168.0, 137.4, 129.1, 128.8, 126.9, 61.9, 51.8, 51.5, 33.2, 14.0.

**Diethyl 2-(1-oxonon-6-en-2-yl)propanedioate**

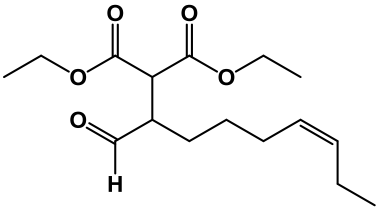

$^1$H NMR (300 MHz, CDCl3) δ 9.70 (d,1H, C**H**O), 5.15-5.36 (m, 2H, $CH_2C\mathbf{H}=C\mathbf{H}CH_2$), 4.09-4.20 (m, 4H, $2\times CO_2C\mathbf{H}_2CH_3$), 3.68, 3.65 (d, 1H, $C\mathbf{H}(CO_2Et)_2$), 3.01-3.08 (m, 1H, CHOC**H**), 1.90-2.01 (m, 4H, $C\mathbf{H}_2CH=CHC\mathbf{H}_2$), 1.26-1.68 (m, 4H, $C\mathbf{H}_2C\mathbf{H}_2CH_2CH=CHCH_2CH_3$), 1.24, 1.22, 1.19, 1.17 (t, 6H, $2\times CO_2CH_2C\mathbf{H}_3$), 0.90, 0.88, 0.85 (t, 3H, $CH_2CHCH=CH_2C\mathbf{H}_3$); $^{13}$C NMR (300 MHz, $CDCl_3$) δ 201.4, 168.1, 167.9, 132.6, 127.8, 61.8, 61.8, 51.8, 50.2, 26.9, 26.6, 26.5, 20.5, 14.3, 14.0, 13.9.

**2-(2-Oxo-2-phenylethyl)hexanal**

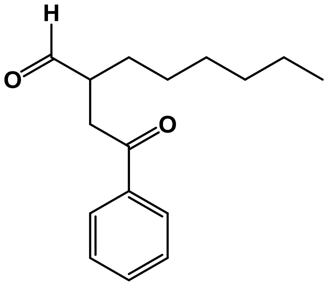

$^1$H NMR (300 MHz, CDCl3) δ 9.76 (d, 1H, C**H**O), 7.89-7.92 (m, 2H, Ar**H**), 7.48-7.53 (m, 1H, Ar**H**), 7.37-7.43 (m, 2H, Ar**H**), 3.37-3.45 (dd, 1H, $C\mathbf{H}_2$COPh), 3.08-3.91 (m, 2H, $C\mathbf{H}_2$COPh & C**H**CHO), 1.67-1.79 (m, 1H, $C\mathbf{H}_2(CH_2)_4CH_3$), 1.42-1.54 (m, 1H, $C\mathbf{H}_2(CH_2)_4CH_3$), 1.15-1.25 (m, 1H, $CH_2(C\mathbf{H}_2)_4CH_3$), 0.79, 0.81, 0.83 (t, 3H, $C\mathbf{H}_3$); $^{13}$C NMR (300 MHz, $CDCl_3$) δ 203.6, 198.0, 136.6, 133.3, 128.6, 128.1, 46.8, 37.7, 31.6, 29.3, 28.9, 27.1, 22.6, 14.0.

**2-(2-(4-Nitrophenyl)-2-oxoethyl)octanal**

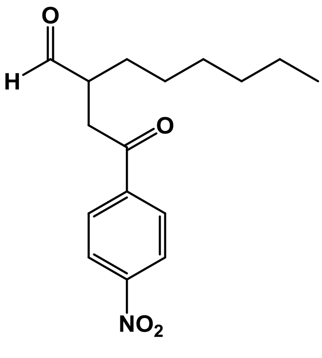

$^1$H NMR (300 MHz, CDCl3) δ 9.74 (s, 1H, C**H**O), 8.24-8.27 (m, 2H, Ar**H**), 8.05-8.08 (m, 2H, Ar**H**), 3.41-3.49 (dd, 1H, $C\mathbf{H}_2$COAr), 3.06-3.15 (m, 1H, CHOC**H**), 2.86-2.93 (dd, 1H, $C\mathbf{H}_2$COAr), 1.71-1.82 (m, 1H, $C\mathbf{H}_2(CH_2)_4CH_3$), 1.44-1.56 (m, 1H, $C\mathbf{H}_2(CH_2)_4CH_3$), 1.23-1.39 (m, 8H, $CH_2(C\mathbf{H}_2)_4CH_3$); $^{13}$C NMR (300 MHz, $CDCl_3$) δ 203.0, 196.7, 150.4, 141.1, 129.1, 123.9, 46.9, 37.8, 31.6, 29.3, 28.7, 27.1, 22.5, 14.0.

## $^1$H and $^{13}$C NMR Spectra of Products

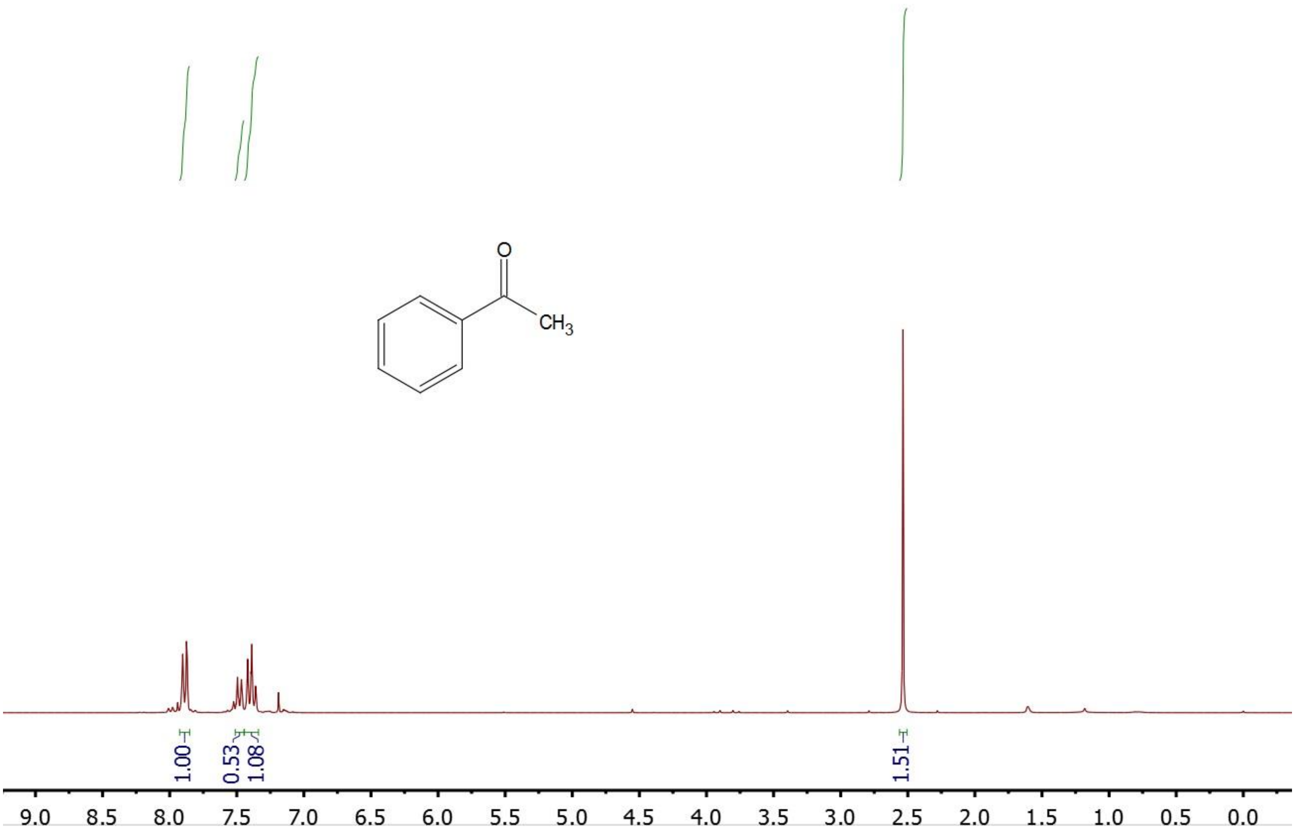

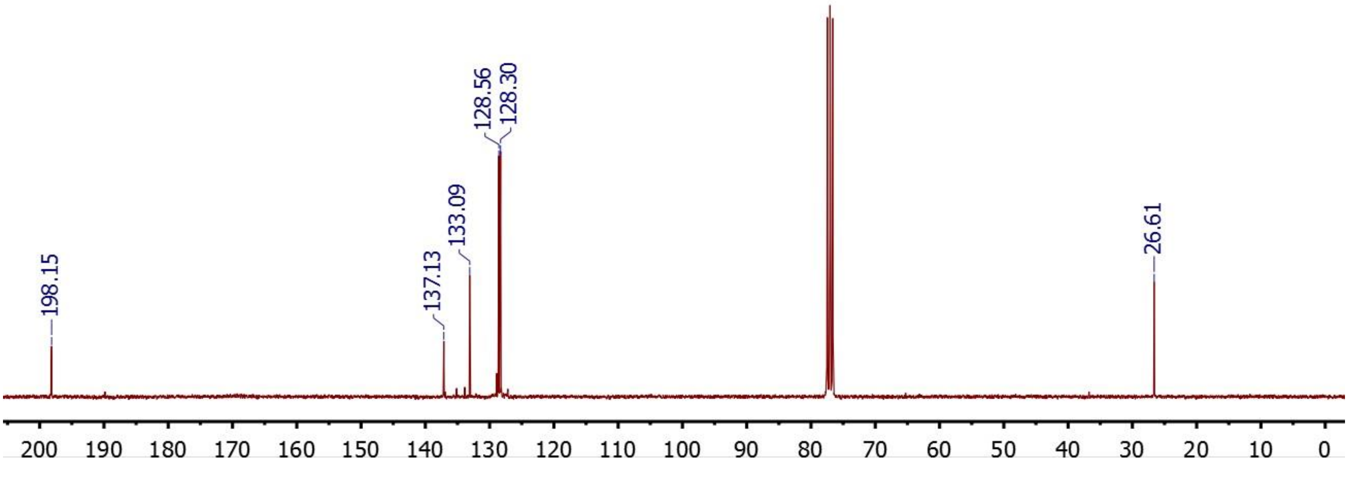

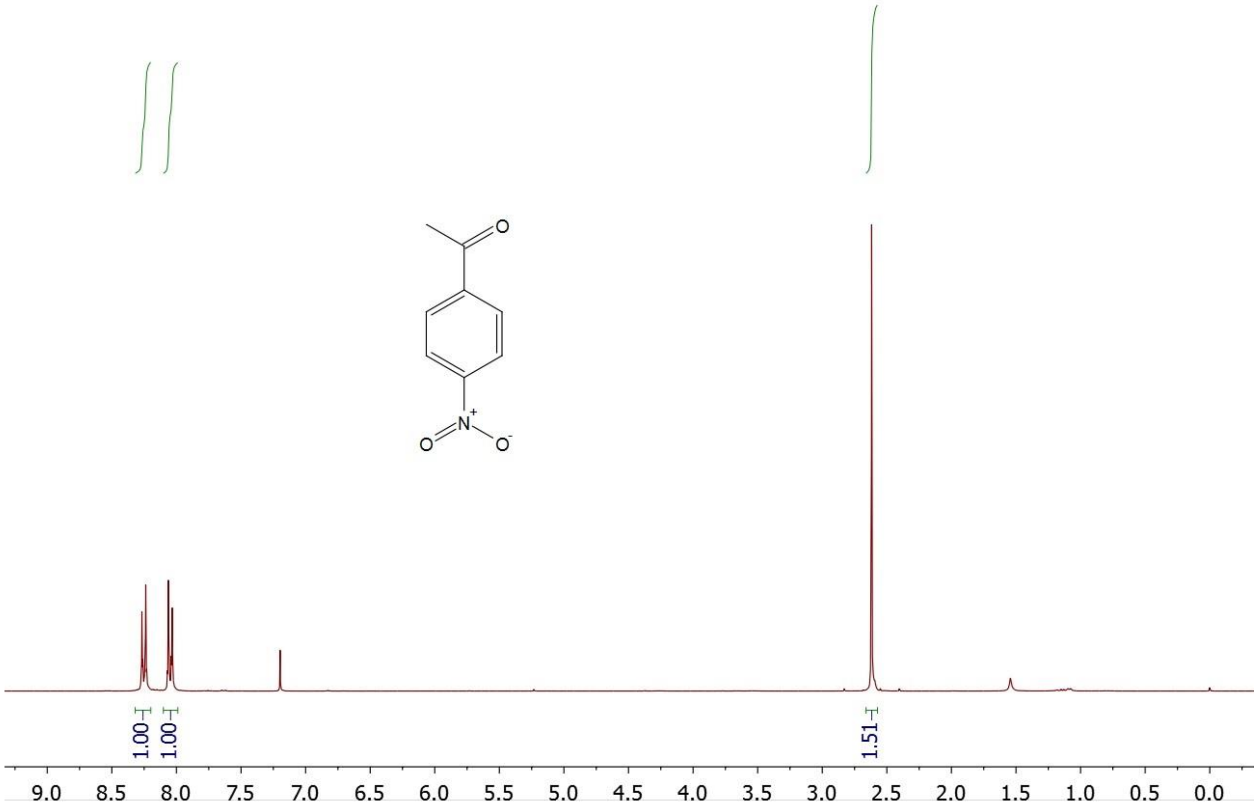
1.00
1.00
1.51
9.0 8.5 8.0 7.5 7.0 6.5 6.0 5.5 5.0 4.5 4.0 3.5 3.0 2.5 2.0 1.5 1.0 0.5 0.0
O
N+
O
O-


196.28
150.37
141.37
129.30
123.86
26.99
210 200 190 180 170 160 150 140 130 120 110 100 90 80 70 60 50 40 30 20 10 0

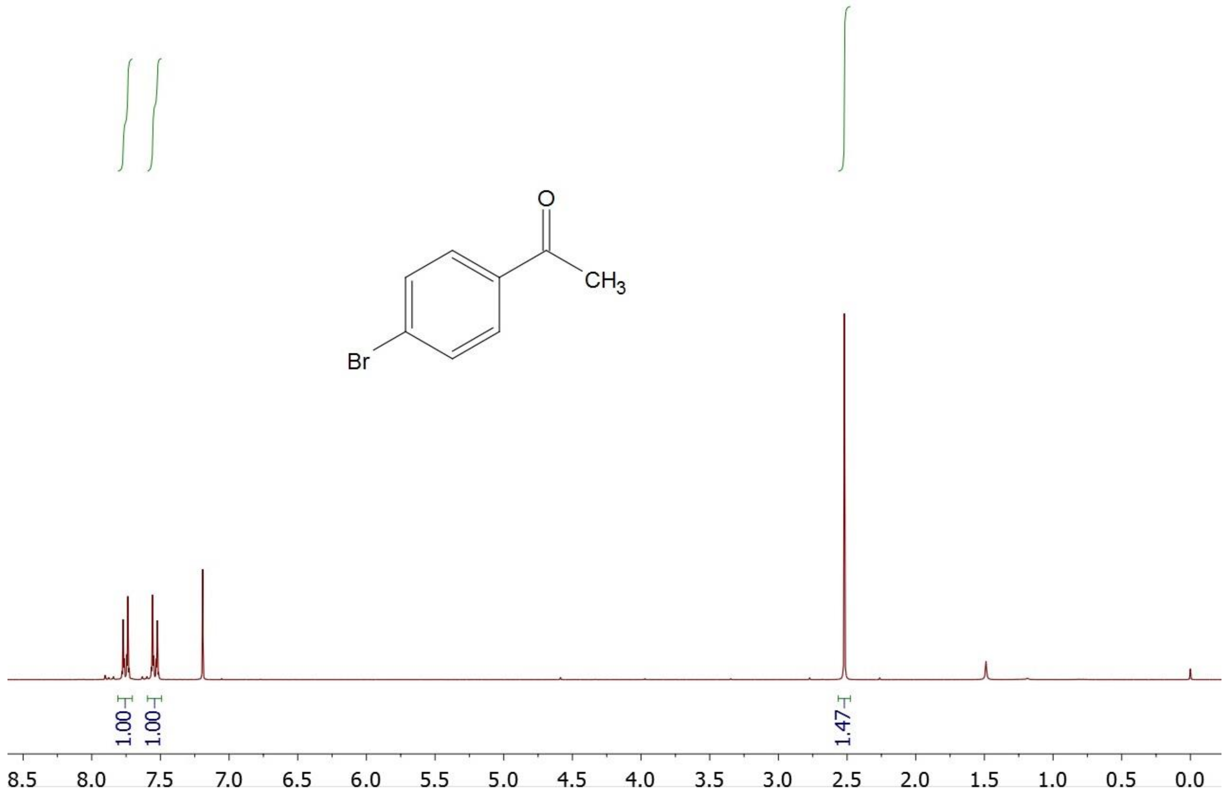
O
CH3
Br
1.00
1.00
1.47
8.5 8.0 7.5 7.0 6.5 6.0 5.5 5.0 4.5 4.0 3.5 3.0 2.5 2.0 1.5 1.0 0.5 0.0

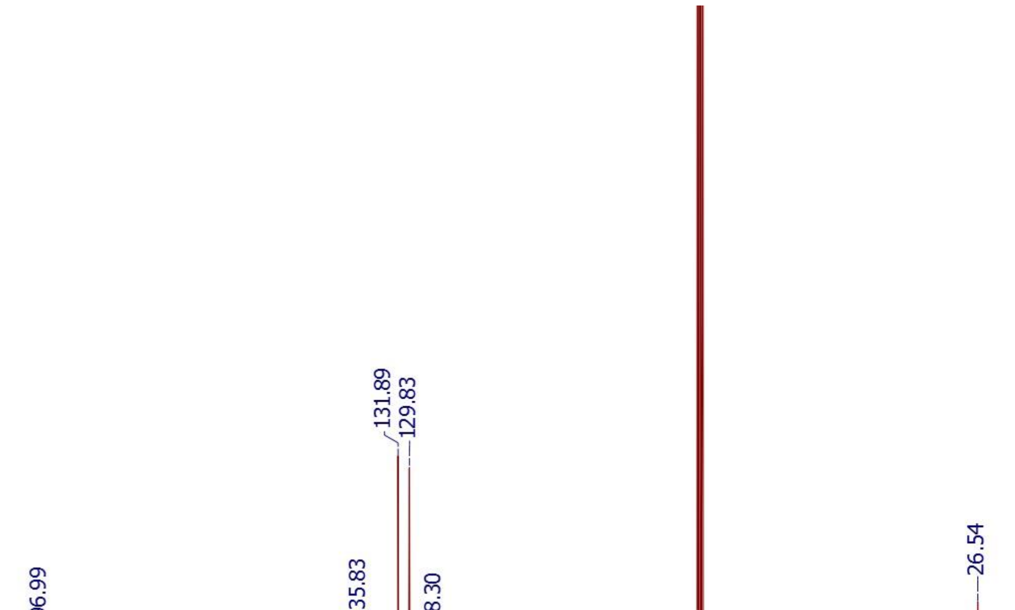
196.99
135.83
131.89
129.83
128.30
26.54
210 200 190 180 170 160 150 140 130 120 110 100 90 80 70 60 50 40 30 20 10 0

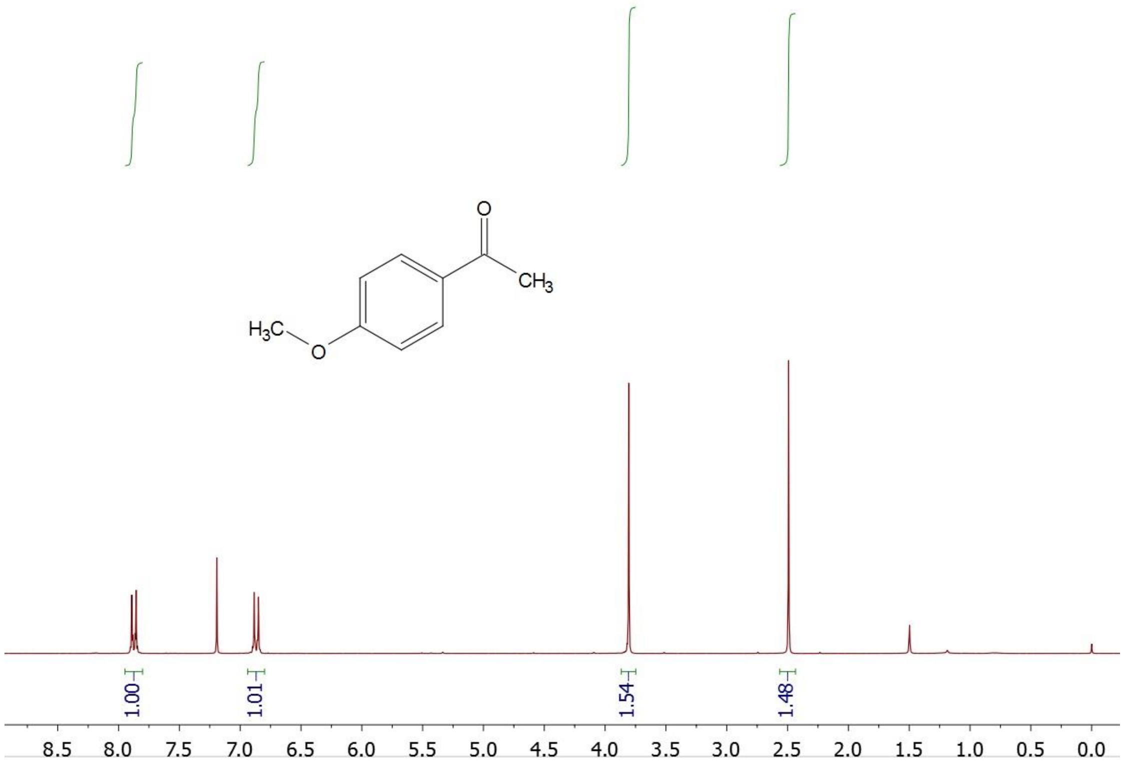
O
CH3
H3C
O
1.00
1.01
1.54
1.48
8.5
8.0
7.5
7.0
6.5
6.0
5.5
5.0
4.5
4.0
3.5
3.0
2.5
2.0
1.5
1.0
0.5
0.0

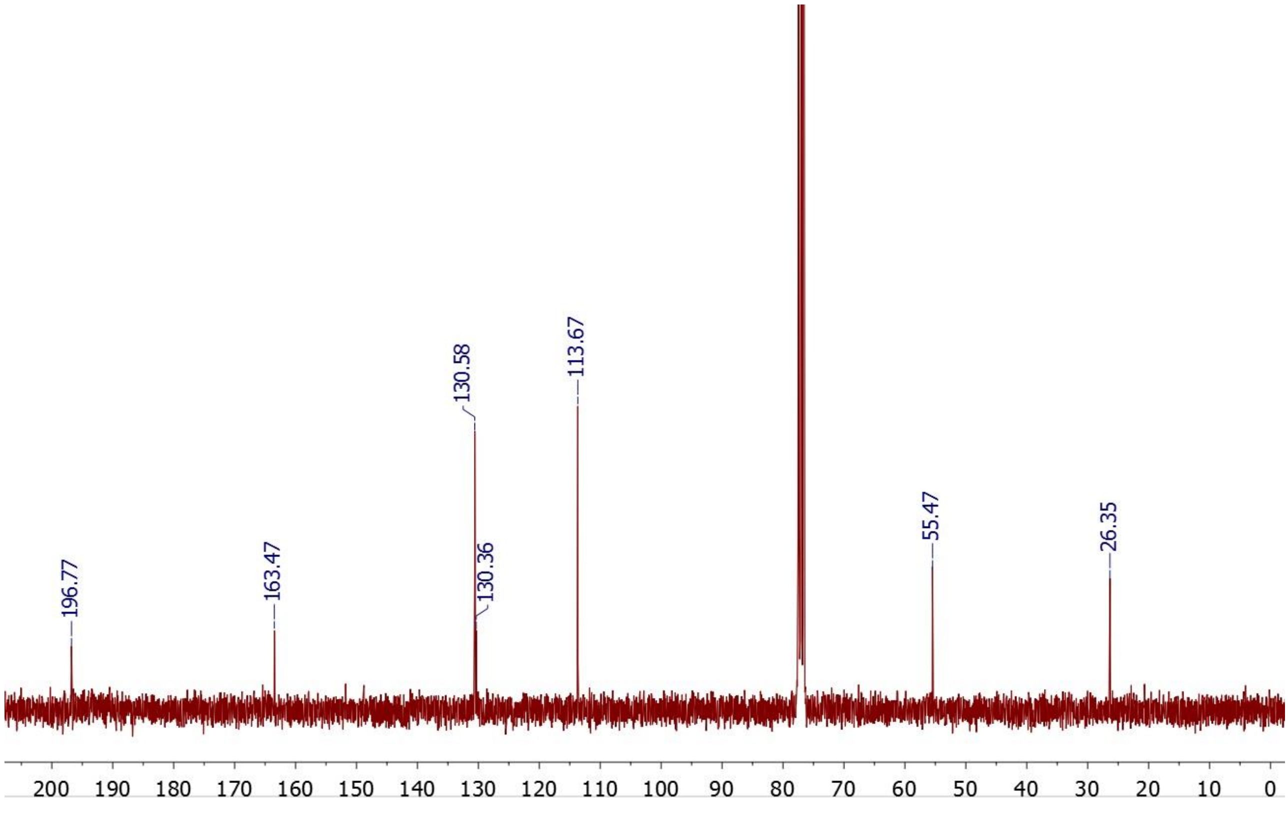
196.77
163.47
130.58
130.36
113.67
55.47
26.35
200
190
180
170
160
150
140
130
120
110
100
90
80
70
60
50
40
30
20
10
0

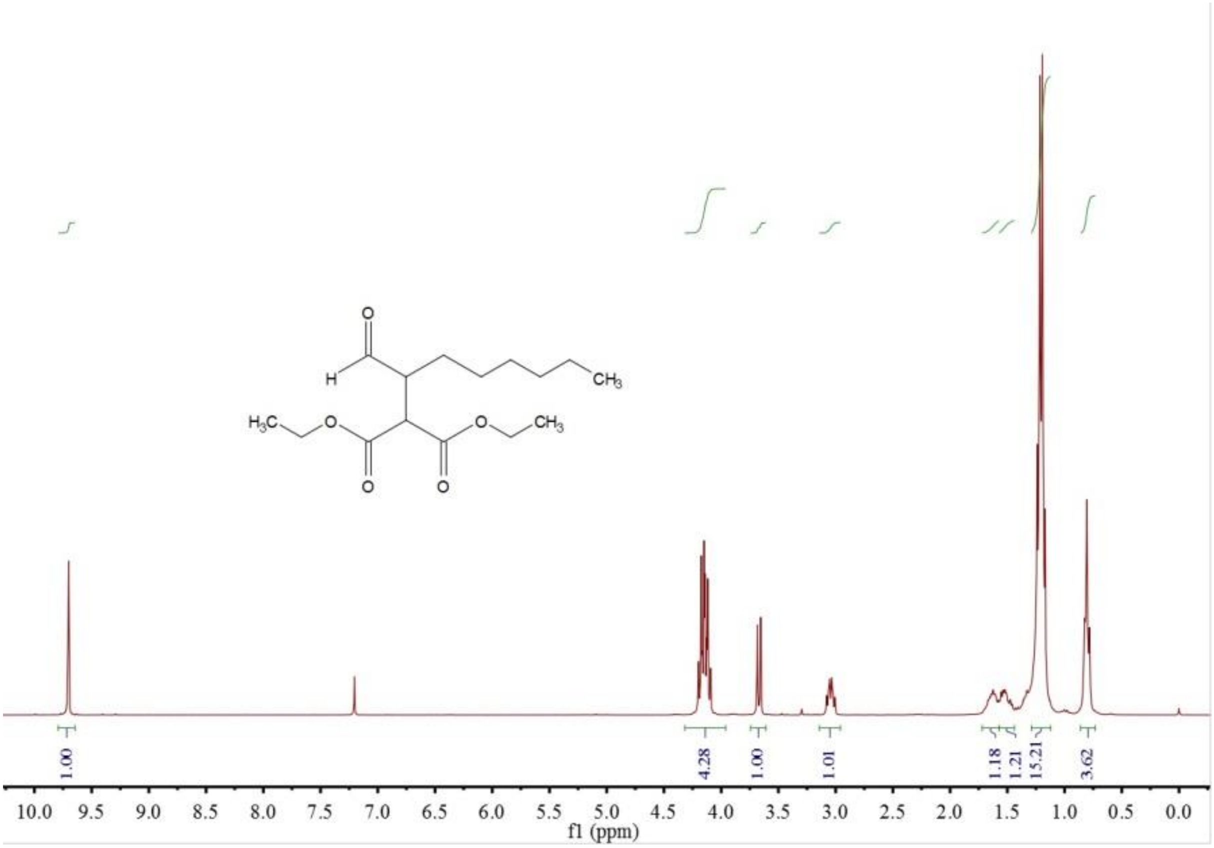
O
H
CH3
H3C
O
O
CH3
O
O
1.00
4.28
1.00
1.01
1.18
1.21
15.21
3.62
10.0 9.5 9.0 8.5 8.0 7.5 7.0 6.5 6.0 5.5 5.0 4.5 4.0 3.5 3.0 2.5 2.0 1.5 1.0 0.5 0.0
f1 (ppm)

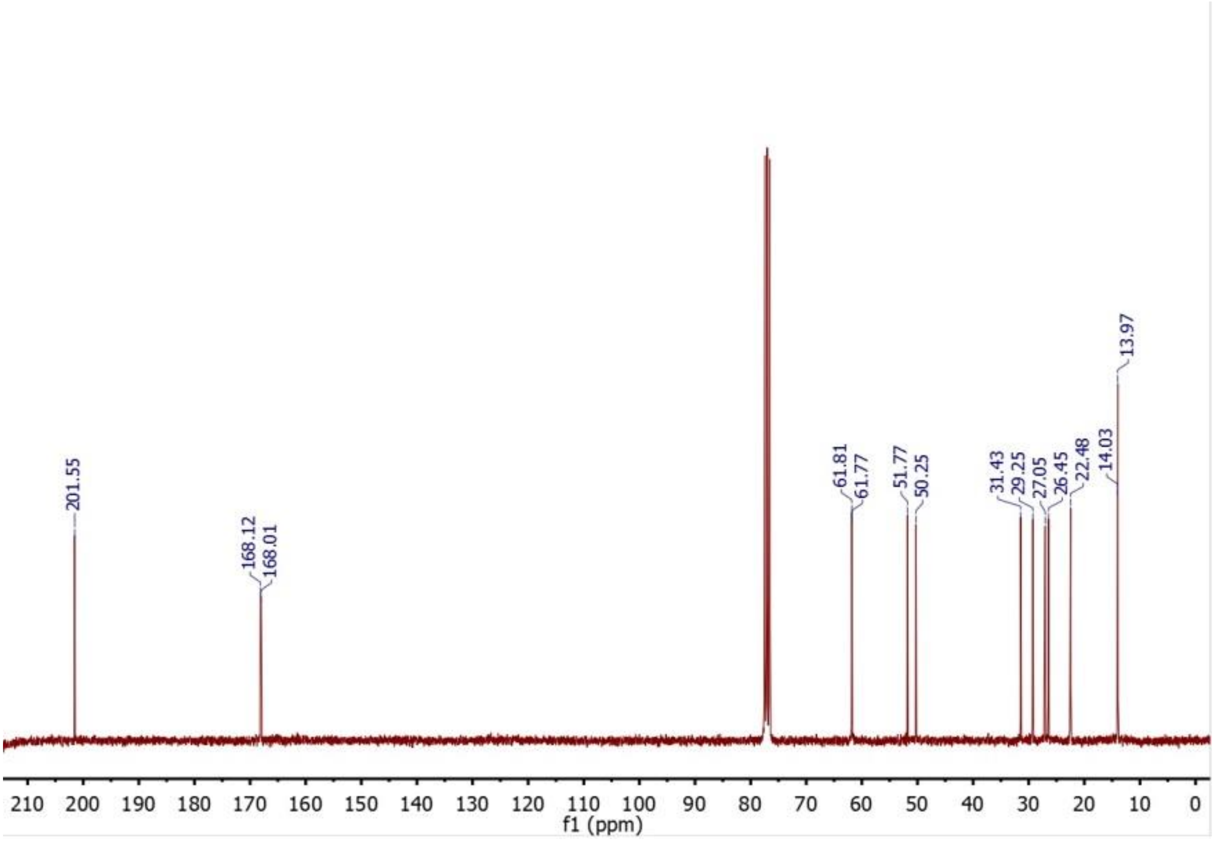
201.55
168.12
168.01
61.81
61.77
51.77
50.25
31.43
29.25
27.05
26.45
22.48
14.03
13.97
210 200 190 180 170 160 150 140 130 120 110 100 90 80 70 60 50 40 30 20 10 0
f1 (ppm)

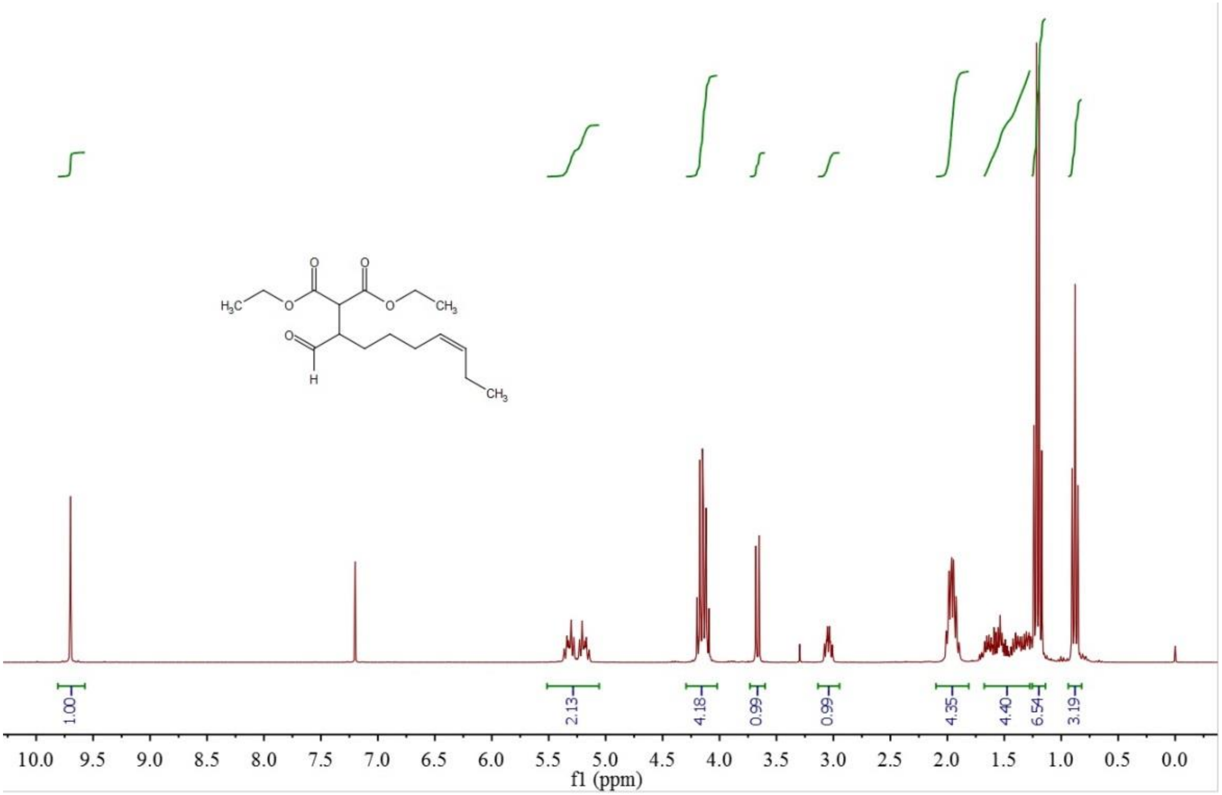
H$_3$C
O
O
O
O
CH$_3$
O
H
CH$_3$
1.00
2.13
4.18
0.99
0.99
4.35
4.40
6.54
3.19
10.0 9.5 9.0 8.5 8.0 7.5 7.0 6.5 6.0 5.5 5.0 4.5 4.0 3.5 3.0 2.5 2.0 1.5 1.0 0.5 0.0
f1 (ppm)

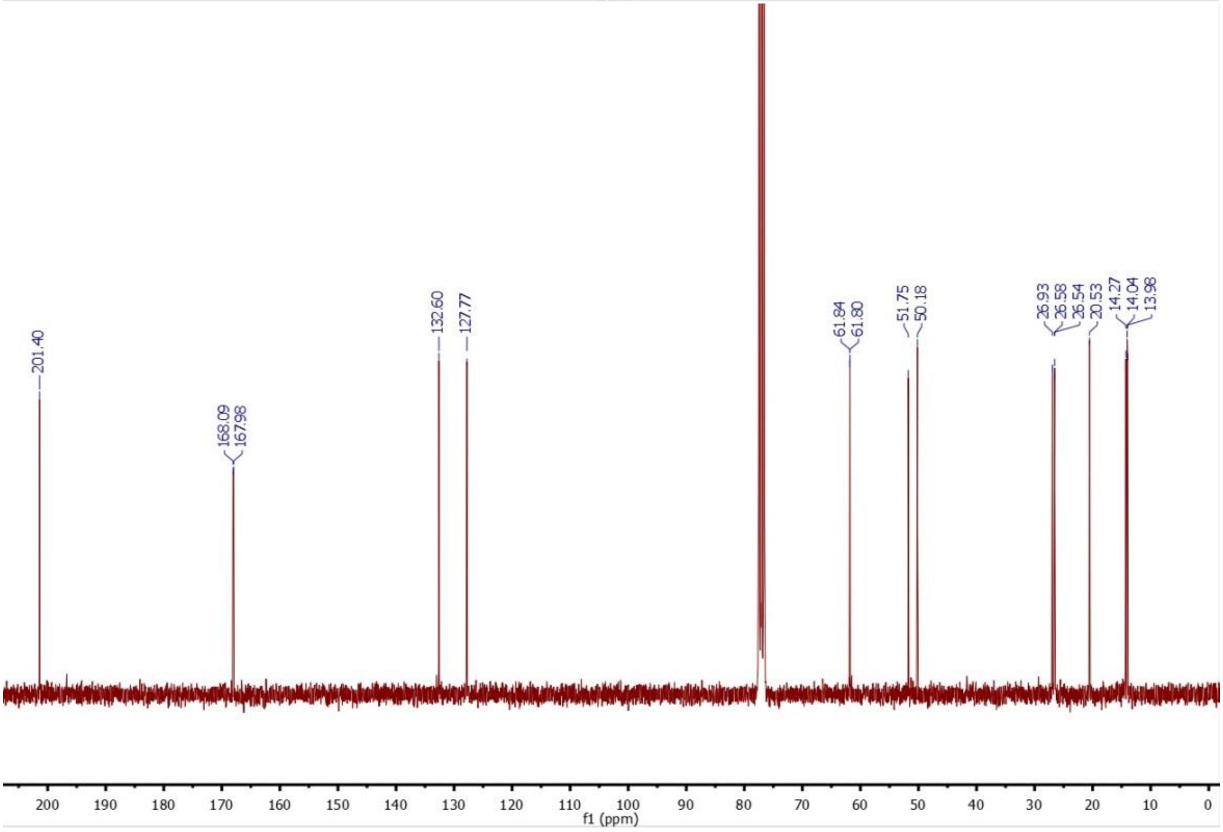
201.40
168.09
167.98
132.60
127.77
61.84
61.80
51.75
50.18
26.93
26.58
26.54
20.53
14.27
14.04
13.98
200 190 180 170 160 150 140 130 120 110 100 90 80 70 60 50 40 30 20 10 0
f1 (ppm)

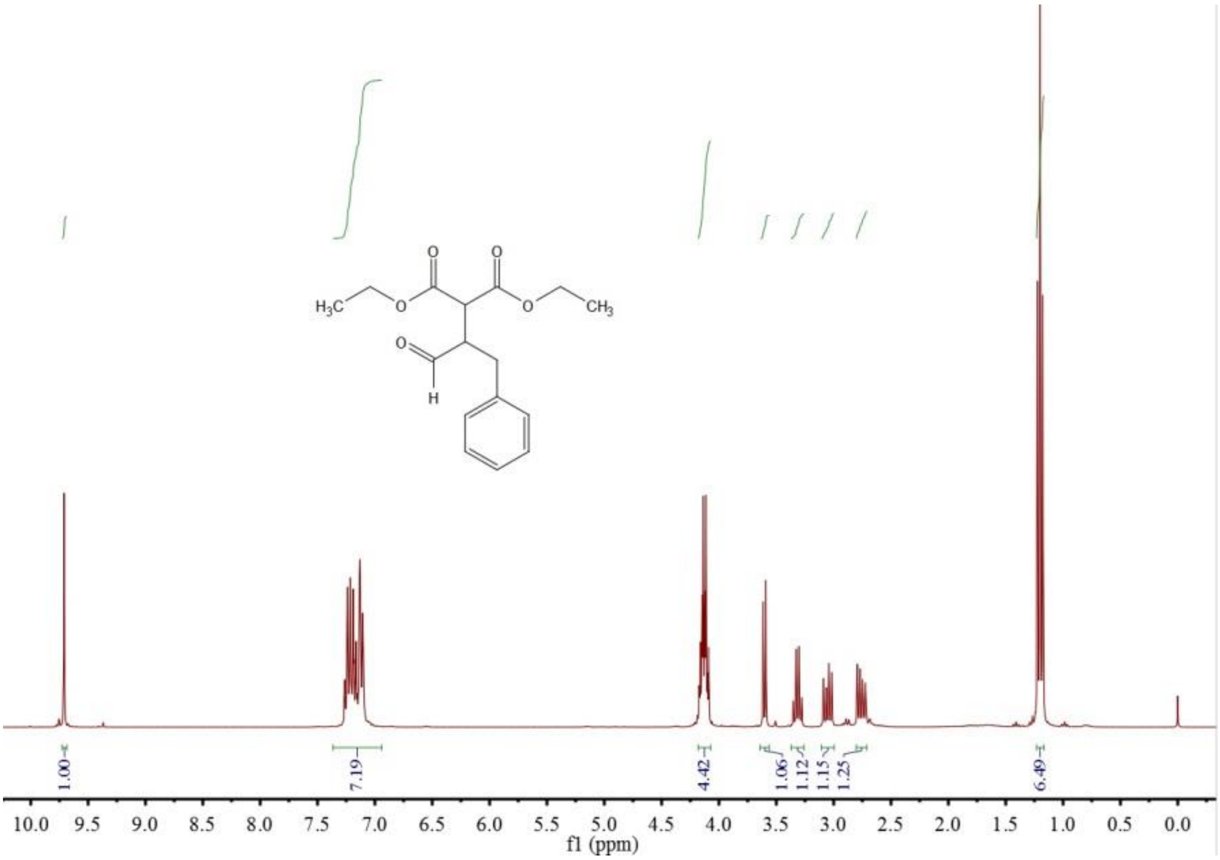
O
O
H3C
O
O
CH3
O
H
1.00
7.19
4.42
1.06
1.12
1.15
1.25
6.49
10.0
9.5
9.0
8.5
8.0
7.5
7.0
6.5
6.0
5.5
5.0
4.5
4.0
3.5
3.0
2.5
2.0
1.5
1.0
0.5
0.0
f1 (ppm)

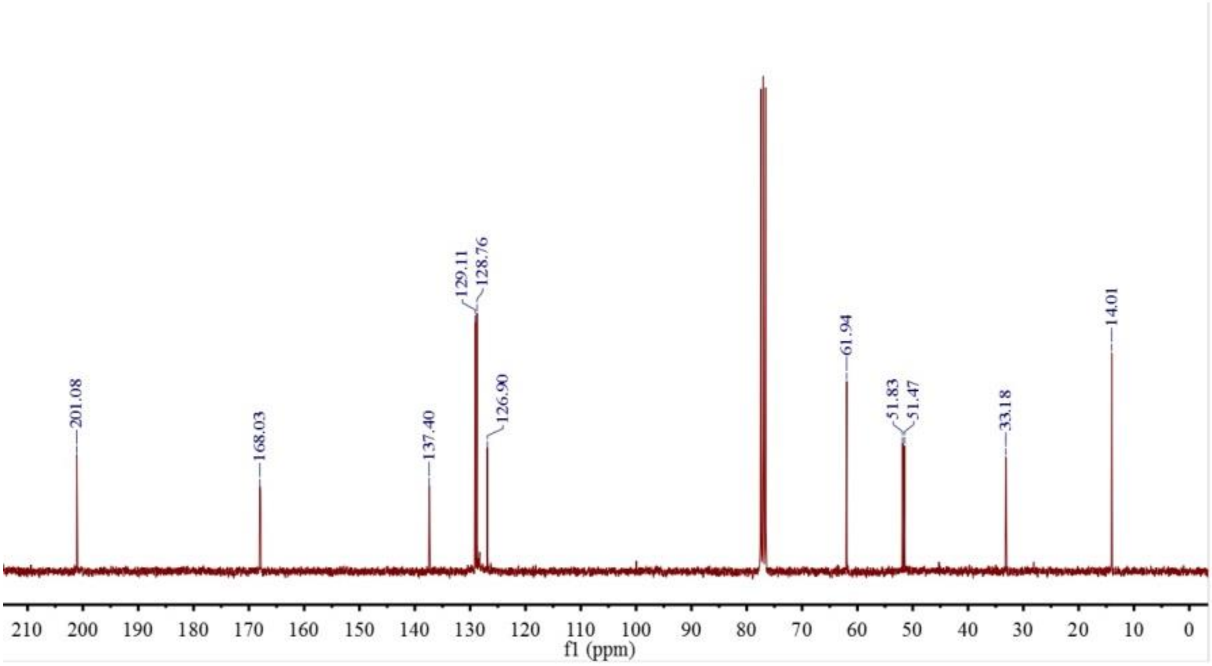
201.08
168.03
137.40
129.11
128.76
126.90
61.94
51.83
51.47
33.18
14.01
210
200
190
180
170
160
150
140
130
120
110
100
90
80
70
60
50
40
30
20
10
0
f1 (ppm)

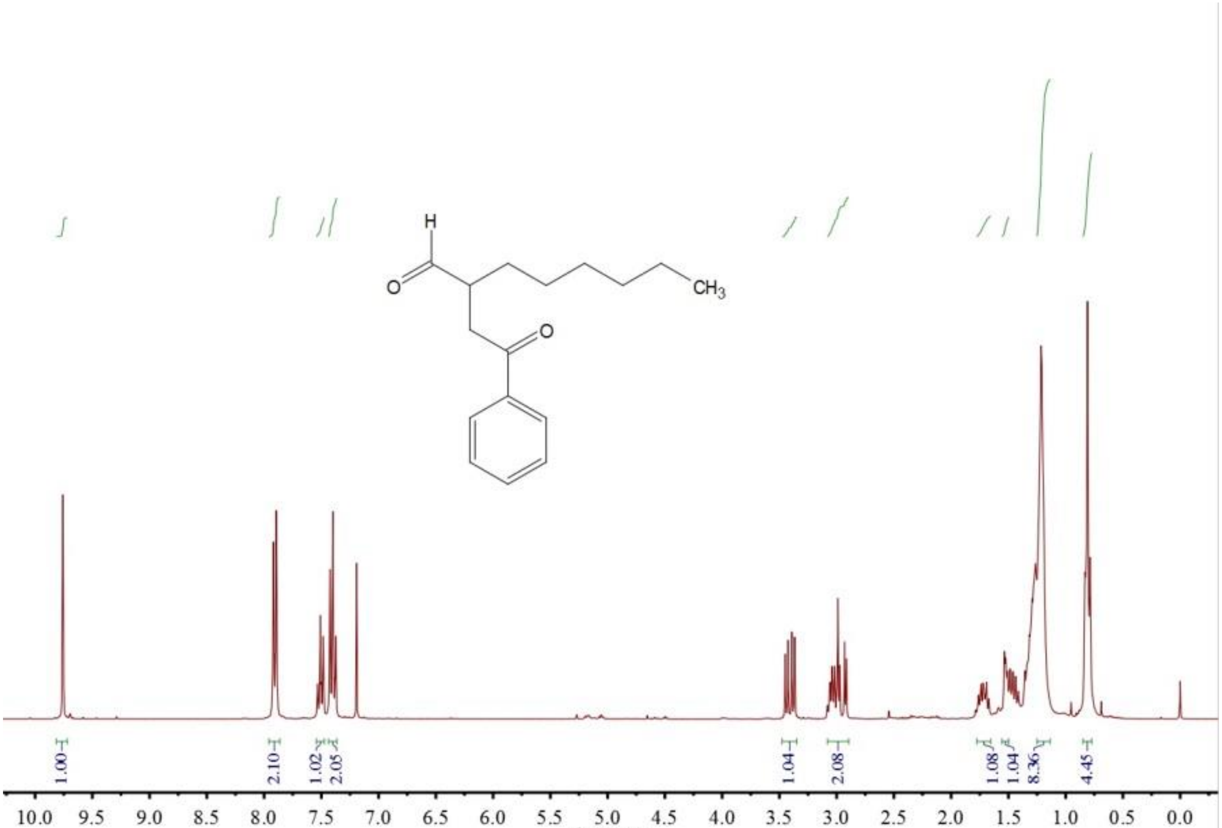
H
O
O
CH3
1.00
2.10
1.02
2.05
1.04
2.08
1.08
1.04
8.36
4.45
10.0 9.5 9.0 8.5 8.0 7.5 7.0 6.5 6.0 5.5 5.0 4.5 4.0 3.5 3.0 2.5 2.0 1.5 1.0 0.5 0.0
f1 (ppm)

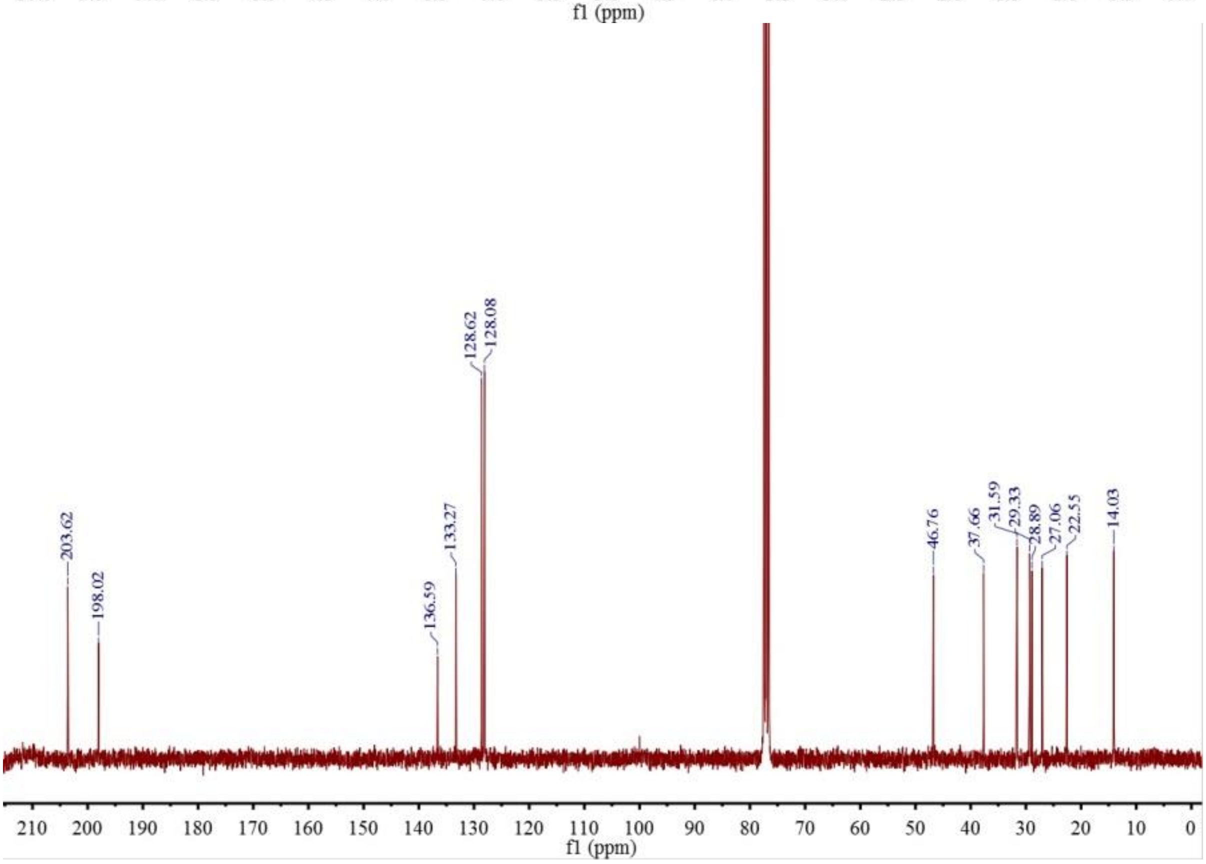
203.62
198.02
136.59
133.27
128.62
128.08
46.76
37.66
31.59
29.33
28.89
27.06
22.55
14.03
210 200 190 180 170 160 150 140 130 120 110 100 90 80 70 60 50 40 30 20 10 0
f1 (ppm)

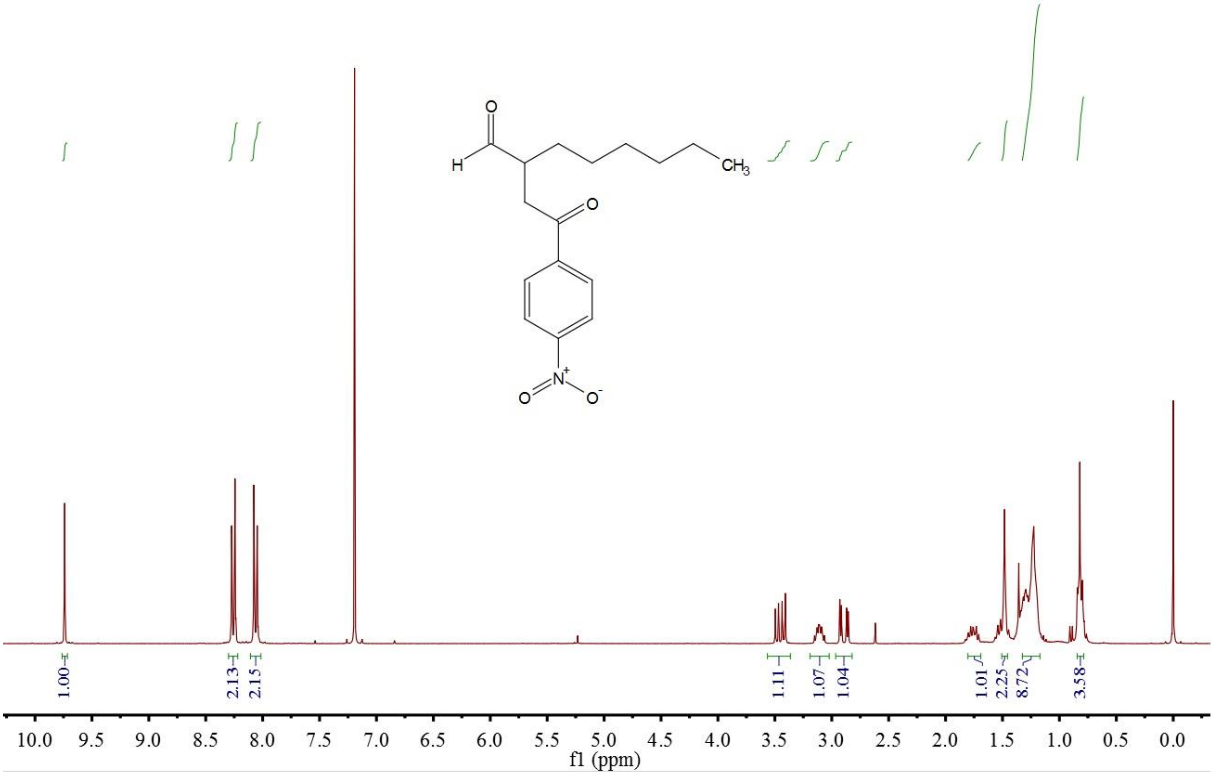
O
H
CH3
O
N+
O-
O
1.00
2.13
2.15
1.11
1.07
1.04
1.01
2.25
8.72
3.58
10.0
9.5
9.0
8.5
8.0
7.5
7.0
6.5
6.0
5.5
5.0
4.5
4.0
3.5
3.0
2.5
2.0
1.5
1.0
0.5
0.0
f1 (ppm)

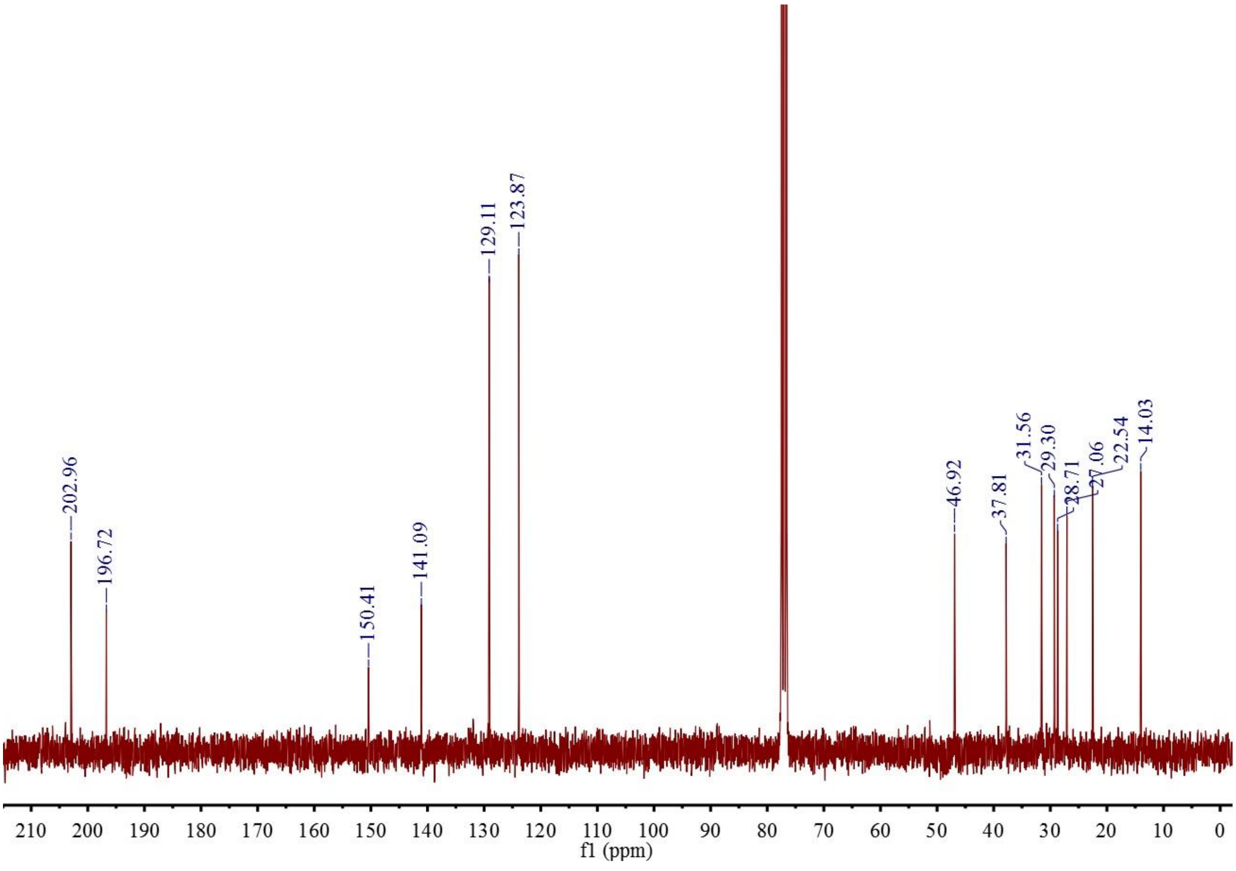
202.96
196.72
150.41
141.09
129.11
123.87
46.92
37.81
31.56
29.30
28.71
27.06
22.54
14.03
210
200
190
180
170
160
150
140
130
120
110
100
90
80
70
60
50
40
30
20
10
0
f1 (ppm)